DMD Fast Forward. Published on August 22, 2018 as DOI: 10.1124/dmd.118.083246
This article has not been copyedited and formatted. The final version may differ from this version.

DMD # 83246

Application of Intestinal Epithelial Cells Differentiated from Human Induced Pluripotent Stem Cells for Studies of Prodrug Hydrolysis and Drug Absorption in the Small Intestine

Takanori Akazawa, Shinpei Yoshida, Shuichi Ohnishi, Takushi Kanazu, Makoto Kawai, and Koji Takahashi

Research Laboratory for Development, Shionogi & Co., Ltd. (T.A., S.Y., S.O., T.K.), Medicinal Chemistry Research Laboratory, Shionogi & Co., Ltd. (M.K.), Drug Discovery & Disease Research Laboratory, Shionogi & Co., Ltd. (K.T.)

Running title: Hydrolysis and Absorption in iPS Cell-Derived Enterocytes

Corresponding Author:

Takanori Akazawa

Research Laboratory for Development, Shionogi & Co., Ltd.

3-1-1, Futaba-cho, Toyonaka, Osaka 561-0825, Japan

Email: takanori.akazawa@shionogi.co.jp

Phone: +81-6-6331-8046

Fax: +81-6-6331-8900

Number of text pages: 30

Number of tables: 6 Supplemental

Number of figures: 6 + 4 Supplemental

Number of references: 45 + 7 Supplemental

Number of words in Abstract: 220

Number of words in Introduction: 610

Number of words in Discussion: 1486

ABBREVIATIONS:

AUC, area under the plasma concentration-time curve; BA, bioavailability; BCRP, breast cancer resistance protein; CDX2, caudal type homeobox 2; CES, carboxylesterase; CHGA, chromogranin A; CYP, cytochrome P450; DE, definitive endoderm; EGF, epidermal growth factor; FGF, fibroblast growth factor; FOXA2, forkhead box protein A2; GAPDH, glyceraldehyde-3-phosphate dehydrogenase; GATA4, GATA binding protein 4; HG, hindgut; hiPSCs, human induced pluripotent

stem cells; hiPSC-IECs; human induced pluripotent stem cell derived intestinal epithelial cells; ISX, intestine specific homeobox; LGR5, leucine rich repeat containing G protein-coupled receptor 5; LC/MS/MS, liquid chromatography/tandem mass spectrometry; LYZ, lysozyme; MACS, magnetic activated cell sorting; MUC2, mucin 2; OCT3/4, octamer-binding transcription factor 3/4; qPCR, quantitative polymerase chain reaction; PEPT1, peptide transporter 1; P-gp, P-glycoprotein; SI, sucrase-isomaltase; SOX, SRY (sex determining region Y)-box; TFF3, trefoil factor 3; UGT, UDP-glucuronosyltransferase; VIL, villin-1.

ABSTRACT

Cell models to investigate intestinal absorption functions, such as of transporters and metabolic enzymes, are essential for oral drug discovery and development. The purpose of this study was to generate intestinal epithelial cells from human induced pluripotent stem cells (hiPSC-IECs) and then clarify whether the functions of hydrolase and transporters in them reflect oral drug absorption in the small intestine. The hiPSC-IECs showed the transport activities of P-gp, BCRP, and PEPT1, revealed by using their probe substrates ([^{3}H]digoxin, sulfasalazine, and [^{14}C]glycylsarcosine), and the metabolic activities of CYP3A4, CES2, and CES1, which were clarified using their probe substrates (midazolam, irinotecan, and temocapril). The intrinsic clearance of hydrolysis of six ester prodrugs into the active form in hiPSC-IECs was correlated with the plasma exposure (C_{max}, AUC, and bioavailability) of the active form after oral administration of these prodrugs to rats. Also, the permeability coefficients of 14 drugs, containing two substrates of P-gp (doxorubicin and [^{3}H]digoxin), one substrate of BCRP (sulfasalazine), and 11 non-substrates of transporters (ganciclovir, [^{14}C]mannitol, famotidine, sulpiride, atenolol, furosemide, ranitidine, hydrochlorothiazide, acetaminophen, propranolol, and antipyrine), in hiPSC-IECs were correlated with their values of the fraction of intestinal absorption (Fa) in human clinical studies. These findings suggest that hiPSC-IECs would be a useful cell model to investigate the hydrolysis of ester prodrugs and to predict drug absorption in the small intestine.

Introduction

Successful prediction of human intestinal absorption can help minimize the number of drug candidates dropped due to pharmacokinetic problems during human clinical phase studies of oral drug discovery and development. Oral drug absorption is influenced by transporters and metabolic enzymes expressed in intestinal epithelial cells. P-gp and BCRP are important efflux transporters in the small intestine, and there is some clinical relevance of the oral absorption of substrates of these transporters, such as digoxin, fexofenadine, aliskiren, dabigatran (P-gp substrates), sulfasalazine, atorvastatin, and rosuvastatin (BCRP substrates), being restricted by efflux transport via these transporters (Simpson and Jarvis, 2000; Fenner et al., 2009; Keskitalo et al., 2009; Tapaninen et al., 2011; Delavenne et al., 2012; Kusuhara et al., 2012). PEPT1 is also involved in transport from the intestinal lumen into epithelial cells of β-lactam antibiotics and ACE inhibitors (Rubio-Aliaga and Daniel, 2008). In addition to transporters, of all CYP isoforms, CYP3A4 is the most abundantly expressed in human small intestine and contributes to the intestinal first-pass metabolism of many substrates, such as midazolam and nifedipine (Rashid et al., 1995; Paine et al., 1996; Paine et al., 2006; Groer et al., 2014; Miyauchi et al., 2016; Akazawa et al., 2018). CES2 is also an important hydrolytic enzyme in the small intestine involved in converting an ester prodrug, such as irinotecan, into its active form (Humerickhouse et al., 2000). To properly predict human intestinal drug absorption from in vitro assessment, a comprehensive cell model of the functions of transporters and metabolic enzymes in human small intestine is desirable.

Caco-2 cells, a human colon carcinoma cell line, have been widely used to predict the fraction of intestinal absorption (Fa) in humans during drug discovery and

development. However, it is difficult to investigate the intestinal first-pass metabolism because Caco-2 cells do not express metabolic enzymes, such as CYP3A4 (Prueksaritanont et al., 1996; Taipalensuu et al., 2001). Furthermore, Caco-2 cells also show different expression patterns of CES isozymes compared with those in the human small intestine; CES2 is more highly expressed than CES1 in human small intestine, whereas CES1 is more highly expressed than CES2 in Caco-2 cells (Imai et al., 2005). Thus, hydrolysis of CES1 substrates, such as temocapril and dabigatran etexilate, has been reported to be overestimated in Caco-2 cells compared to human small intestine (Imai et al., 2005; Ishiguro et al., 2013). These findings show the risk of mistaken prediction of oral absorption of prodrugs.

In recent years, several researchers have succeeded in generating intestinal epithelial cells from human induced pluripotent stem cells (hiPSCs) (Spence et al., 2011; Kauffman et al., 2013; Ogaki et al., 2013; Forbester et al., 2015; Iwao et al., 2015; Ozawa et al., 2015; Uchida et al., 2017). Human induced pluripotent stem cell-derived intestinal epithelial cells (hiPSC-IECs) would be a good tool to predict the absorption of oral drugs in humans, because they are reported to have the functions of transporters, such as BCRP and PEPT1, as well as of metabolic enzymes, such as CYP3A4 and CES2 (Iwao et al., 2015; Ogaki et al., 2015; Ozawa et al., 2015; Kodama et al., 2016; Kabeya et al., 2017; Uchida et al., 2017). Unlike Caco-2 cells, hiPSC-IECs show an expression pattern of CES isozymes similar to the human small intestine; CES2 is expressed at higher levels than CES1 (Kabeya et al., 2017). This suggests that hiPSC-IECs would be more useful than Caco-2 cells for investigating the intestinal hydrolysis of CES substrates, such as ester prodrugs, but it is unknown whether the hydrolysis in hiPSC-IECs reflects the in vivo function of intestinal hydrolysis. In

DMD Fast Forward. Published on August 22, 2018 as DOI: 10.1124/dmd.118.083246
This article has not been copyedited and formatted. The final version may differ from this version.

addition, Kodama et al. demonstrated that the permeabilities across hiPSC-IEC monolayers via passive diffusion were correlated with Fa values in humans (Kodama et al., 2016), but it has not been clarified whether human intestinal absorption of substrates for transporters can be accurately predicted by using hiPSC-IECs.

Therefore, the purpose of this study was to generate hiPSC-IECs and to find whether the functions of hydrolase and transporters in hiPSC-IECs can reflect oral drug absorption in the small intestine. First, the in vitro hydrolysis activities of ester prodrugs in hiPSC-IECs was compared with the plasma exposures (C_{max}, AUC, and BA) of the active form in rats as they are relevant to in vivo hydrolysis activities. Second, the permeabilities of 14 drugs, containing two substrates of P-gp (doxorubicin and [^{3}H]digoxin), one substrate of BCRP (sulfasalazine), and 11 non-substrates of transporters (ganciclovir, [^{14}C]mannitol, famotidine, sulpiride, atenolol, furosemide, ranitidine, hydrochlorothiazide, acetaminophen, propranolol, and antipyrine), were compared with human Fa values.

Materials and Methods

Materials. A human iPS cell line (TkDA3-4) established as described previously (Takayama et al., 2010), was graciously provided by Dr. Makoto Otsu (The Institute of Medical Science, The University of Tokyo, Tokyo, Japan). All studies with human iPS cells were approved by the Ethics Committee on Human Tissue and Genome Research at Shionogi & Co., Ltd. (Toyonaka, Japan). The Caco-2 cell line was purchased from the American Type Culture Collection (Rockville, MD). Total RNAs of human adult small intestines pooled from five donors (20-61 years old) and human fetal small intestine from one donor (26 weeks of gestation) were purchased from Clonetech (Palo Alto, CA) and BioChain Institute Inc. (Newark, CA), respectively. Six ester prodrugs (prodrugs A, B, C, D, E, and F) and the active form, candidates for anti-influenza virus agents, were in-house compounds synthesized by Shionogi & Co., Ltd.; these prodrugs are hydrolyzed into the same active form (Fig. S1 and Table S1). All other reagents were of the highest quality available.

Animals. Male Sprague-Dawley (SD) rats (8 weeks of age) were purchased from CLEA Japan Inc. (Osaka, Japan). Rats were maintained on a 12 hr light/dark cycle in a temperature and humidity-controlled environment with free access to food and water. At more than 3 days before the experiment, a cannula tube was inserted into the jugular vein of each rat under ether anesthesia. All animal studies were approved by the Committee for Animal Care and Use at Shionogi & Co., Ltd.

Cultivation of hiPSC-IEC and Caco-2 Cell Monolayers on Transwell Inserts. HiPSC-IECs were generated from hiPSCs according to the preparation methods

DMD Fast Forward. Published on August 22, 2018 as DOI: 10.1124/dmd.118.083246
This article has not been copyedited and formatted. The final version may differ from this version.

as described in the Supplemental Data. Generated hiPSC-IECs were seeded on porous polyester membrane 24 well Transwell inserts (0.4 μm pore size and 0.33 cm^2 filter area) (Corning Inc., Corning, NY) coated with 0.5 mg/ml laminin 511-E8 (iMatrix-511; Nippi, Tokyo, Japan) at a density of 3.0×10^5 cells/cm^2. Cells were cultured with intestinal epithelial cell (IEC) maintenance medium [Advanced DMEM/F12 (Thermo Fisher Scientific, San Jose, CA) supplemented with 500 ng/ml R-spondin 1 (R&D systems, Minneapolis, MN), 100 ng/ml Noggin (R&D systems), 50 ng/ml epidermal growth factor (EGF; R&D systems), 2 mM L-glutamine (Thermo Fisher Scientific), 100 units/ml penicillin-streptomycin (Thermo Fisher Scientific), 15 mM HEPES (Thermo Fisher Scientific), 2% (v/v) B27 supplement (Thermo Fisher Scientific), 1% N2 supplement (Thermo Fisher Scientific), 1 mM N-acetylcysteine (Sigma-Aldrich, St. Louis, MO), 10 nM human gastrin 1 (Peptide Institute, Osaka, Japan), and 500 nM A-83-01 (Tocris, Bristol, UK)] containing 10 μM Y27632 (Wako, Osaka, Japan) for 3 days as described in a previous report (Sato et al., 2011). Next, the medium was changed to IEC maintenance medium without Y27632, and cultured for 20-22 days with medium change every 2 or 3 days.

Caco-2 cells were cultured in DMEM (Thermo Fisher Scientific) supplemented with 10% fetal bovine serum (FBS; Equitech-bio, Kerrville, TX), 1% NEAA, 100 units/ml penicillin-streptomycin, and 6 mM HEPES on a 10 cm culture dish. Cells were harvested with trypsin (0.25%)-EDTA (1 mM) and seeded on porous polyester membrane Transwell filters (0.4 μm pore size and 0.33 cm^2 filter area) at a density of 1.3×10^5 cells/cm^2. The culture medium was replaced every 2 or 3 days.

The resistance (Ω) of hiPSC-IEC and Caco-2 cell monolayers was measured on each Transwell insert by using a Millicell® ERS-2 system (Millipore Corporation,

Bedford, MA), and corrected for background resistance with an insert that did not contain cells. The transepithelial electric resistance (TEER; $\Omega \times cm^2$), an index of the formation of tight junctions, of hiPSC-IEC and Caco-2 cell monolayers, was determined as the product of the resistance (Ω) and the surface area of insert (0.33 cm^2). All cultures were performed at 37°C in a humidified atmosphere of 5% CO_2 and 95% air.

Quantification of Gene Expression of Transporters and Metabolic Enzymes Using a Quantitative Polymerase Chain Reaction (qPCR). Total RNAs of human iPS cells, hiPSC-IECs, and Caco-2 cells were isolated by using a PureLink® RNA Mini Kit (Invitogen, Carlsbad, CA). The qPCR analyses for nine genes [P-gp, BCRP, PEPT1, CYP3A4, CYP3A7, CES1, CES2, UGT1A1, and GAPDH (primer 1)] were performed by means of an Applied Biosystems 7500 Real Time PCR System (Applied Biosystems, Carlsbad, CA) using a TaqMan® Fast Universal PCR Master Mix (Applied Biosystems). Three CYP3A isoforms, CYP3A4, CYP3A5, and CYP3A7, are known to express in human small intestine (Miyauchi et al., 2016). The present study measured the gene expression of CYP3A4 and CYP3A7 as a predominant CYP3A isoform in adult and fetal human small intestine (Shin et al., 2009; Betts et al., 2015; Miyauchi et al., 2016). The cDNA was synthesized with a High-Capacity cDNA Reverse Transcription Kit (Applied Biosystems). The reaction solution for cDNA synthesis consisted of 10 μL of RNA, 2 μL of 10 × RT buffer, 2 μL of 10 × RT random primers, 0.8 μL of 25 × dNTP Mix (100 mM), 1 μL of MultiScribe reverse transcriptase (50 units/μL), and 4.2 μL of distilled water. The reverse transcription reactions were conducted with an Applied Biosystems 7500 Real Time PCR System under the following conditions: 25°C for 10 min, 37°C for 120 min, and 85°C for 5 min. The

resulting cDNA samples were subjected to qPCR analyses. The reaction solution consisted of 1 μL of cDNA, 1 μL of TaqMan® primer-probe set (Applied Biosystems), 10 μL of 2 × TaqMan® Fast Universal PCR Master Mix, and 8 μL of distilled water. The qPCR reactions were performed under the following conditions: 95°C for 10 sec, followed by 50 cycles of 95°C for 3 sec, 60°C for 30 sec. Information on the TaqMan® primer-probe set is given in Table S2. The expression level of each target gene was normalized relative to that of GAPDH (primer 1). The relative expression of the target gene to GAPDH was calculated using the comparative ΔCt method where ΔCt is obtained by subtracting Ct of GAPDH from the target gene. The relative expression levels of target gene to GAPDH was expressed as $2^{-\Delta Ct}$.

Transcellular Transport Study across hiPSC-IEC and Caco-2 Cell Monolayers. MES transport buffer and HEPES transport buffer were used for transcellular transport experiments. Transport buffers contained 1.26 mM $CaCl_2$, 0.493 mM $MgCl_2$, 0.407 mM $MgSO_4$, 5.33 mM KCl, 0.441 mM KH_2PO_4, 12.8 mM $NaHCO_3$, 138 mM NaCl, 0.338 mM Na_2HPO_4, 30.6 mM D-glucose, 5% FBS, and either 25 mM MES (MES transport buffer) or 25 mM HEPES (HEPES transport buffer). The pH values of the MES transport buffer and HEPES transport buffer were adjusted to 6.0 and 7.4 with NaOH or HCl, respectively. The conditions of transcellular transport studies across hiPSC-IEC or Caco-2 cell monolayers are described in Subsections 1-5.

Subsection 1: Transport Activities of P-gp and BCRP in hiPSC-IEC Monolayers. The functions of P-gp and BCRP were examined by means of bi-directional (apical-to-basolateral and basolateral-to-apical) transcellular transport

studies in hiPSC-IEC monolayers. The functional assessments of P-gp and BCRP were not performed in Caco-2 cell monolayers in the present study. [^{3}H]Digoxin (1 μM, 1.0 μCi/ml) and cyclosporin A (10 μM) were used as a probe substrate and an inhibitor for P-gp, respectively, and sulfasalazine (2 μM) and KO143 (0.1 μM) were used as a probe substrate and an inhibitor for BCRP, respectively. Prior to the transcellular transport experiments, both sides of the cell monolayers were preincubated with HEPES transport buffer in the presence or absence of each transporter inhibitor for 30 min. After pre-incubation, the transport experiment was initiated by replacement with HEPES transport buffer containing each transporter substrate in the presence or absence of each transporter inhibitor on the donor side, and replacement without each transporter substrate in the presence or absence of each transporter inhibitor on the receiver side. The cell monolayers were incubated at 37°C under gentle shaking with a horizontal rotary shaker (MMS-1; EYELA, Tokyo, Japan). Aliquots of solution were collected from the receiver compartment 1, 2, and 3 hr after adding each probe substrate, and the same volume of fresh transport buffer was immediately added except for the sampling at 3 hr.

The apparent permeability coefficient (P_{app}) (cm/sec) of each compound was calculated according to the following equation:

$$P_{app} = \frac{dQ}{dt} \times \frac{1}{A \times C_0} \quad \text{(Eq. 1)}$$

where dQ/dt (pmol/sec) is the flux rate of the test compound across the monolayer and is determined by the slope of the plots of the cumulative permeated amount on the

DMD Fast Forward. Published on August 22, 2018 as DOI: 10.1124/dmd.118.083246
This article has not been copyedited and formatted. The final version may differ from this version.

receiver side versus time using linear regression analysis of the transcellular transport. A is the surface area of the monolayer (0.33 cm^2), and C_0 (pmol/μL) is the initial concentration of test compounds on the donor side.

The contributions of efflux activities of P-gp and BCRP were defined by the efflux ratio as follows:

$$\text{Efflux ratio} = \frac{P_{app,\ b\ to\ a}}{P_{app,\ a\ to\ b}} \quad \text{(Eq. 2)}$$

where $P_{app,\ b\ to\ a}$ (cm/sec) and $P_{app,\ a\ to\ b}$ (cm/sec) represent the apparent permeability coefficients in the basolateral-to-apical direction and apical-to-basolateral direction, respectively.

Subsection 2: Transport Activities of PEPT1 in hiPSC-IEC Monolayers. The function of PEPT1 was examined by means of uni-directional (apical-to-basolateral) transcellular transport studies. The basolateral-to-apical transcellular transport studies were not performed in hiPSC-IEC monolayers. In this study, the function of PEPT1 was not also examined in Caco-2 cell monolayers. Prior to transcellular transport experiments, cell monolayers were pre-incubated with MES transport buffer on the apical side and with HEPES transport buffer on the basolateral side in the presence or absence of a PEPT1 inhibitor (10 mM unlabeled glycylsarcosine) for 30 min, respectively. The transport experiment was initiated by replacement with MES transport buffer containing [^{14}C]glycylsarcosine (10 μM, 1.0 μCi/ml), a PEPT1 substrate, in the presence or absence of 10 mM unlabeled glycylsarcosine on the apical

DMD Fast Forward. Published on August 22, 2018 as DOI: 10.1124/dmd.118.083246
This article has not been copyedited and formatted. The final version may differ from this version.

side, and with HEPES transport buffer without [^{14}C]glycylsarcosine in the presence or absence of 10 mM unlabeled glycylsarcosine on the basolateral side. The cell monolayers were incubated at 37°C under gentle shaking with a horizontal rotary shaker (MMS-1). The aliquots of solution were collected from the basolateral side 1, 2, and 3 hr after adding [^{14}C]glycylsarcosine, and then the same volume of fresh transport buffer was immediately added except for the sampling at 3 hr. The values of P_{app} (cm/sec) of [^{14}C]glycylsarcosine across hiPSC-IEC monolayers were determined according to Eq.1.

Subsection 3: Metabolic Activities of CYP3A4, CES2, and CES1 in hiPSC-IEC and Caco-2 Cell Monolayers. The functions of CYP3A4, CES2, and CES1 were examined by means of uni-directional (apical-to-basolateral) transcellular transport studies performed under the same conditions as described in Subsection 2 except for sampling times. Cells were preincubated with each metabolic enzyme inhibitor [0.5 μM or 10 μM ketoconazole (a CYP3A4 inhibitor), 100 μM telmisartan (a CES2 inhibitor), or 500 μM bis-*p*-nitrophenyl phosphate (BNPP) (a CES inhibitor)] for 30 min. The pre-incubation buffer was replaced with MES transport buffer containing each metabolic enzyme substrate [2 μM midazolam (a CYP3A4 substrate), 100 μM irinotecan (a CES2 substrate), or 100 μM temocapril (a CES1 substrate)] in the presence or absence of each metabolic enzyme inhibitor as described above on the donor side, and replaced with HEPES transport buffer without each metabolic enzyme substrate in the presence or absence of each metabolic enzyme inhibitor on the receiver side. The aliquots of solution were collected from the apical and basolateral compartments 2 hr after adding each probe substrate, and cell monolayers were washed with HEPES transport buffer, then test substrates in the cells were extracted with acetonitrile.

DMD Fast Forward. Published on August 22, 2018 as DOI: 10.1124/dmd.118.083246
This article has not been copyedited and formatted. The final version may differ from this version.

The contribution of drug metabolism to drug permeation across the cell monolayer was defined by the extraction ratio proposed (Fisher et al., 1999). The extraction ratio (%) was calculated according to the following equation:

$$\text{Extraction ratio} = \frac{\sum \text{metabolite}_{(\text{AP, BL, Cell})}}{\sum \text{parent}_{(\text{BL, Cell})} + \sum \text{metabolite}_{(\text{AP, BL, Cell})}} \times 100 \quad \text{(Eq. 3)}$$

where $\sum \text{parent}_{(\text{BL, Cell})}$ (pmol) is the summed amount of parent compound (midazolam, irinotecan, or temocapril) in basolateral (BL) and intracellular (Cell) compartments at the end of the study, and $\sum \text{metabolite}_{(\text{AP, BL, Cell})}$ (pmol) is the summed amount of the metabolites (1-OH midazolam, SN38, or temocaprilat) in apical (AP), basolateral, and intracellular compartments at the end of the study.

Subsection 4: Hydrolytic Activities of Six Ester Prodrugs in hiPSC-IEC Monolayers. The function was examined by means of uni-directional (apical-to-basolateral) transcellular transport studies across hiPSC-IEC monolayers under the same conditions as described in Subsection 3.

The intrinsic clearance (CL_{int}) (μL/min) of each prodrug was calculated according to the following equation:

$$CL_{int} = \frac{\sum AF_{(\text{AP, BL, Cell})} / t}{C_{0,\ \text{PD(AP)}}} \quad \text{(Eq. 4)}$$

where $\sum AF_{(\text{AP, BL, Cell})}$ (pmol) is the summed amount of the active form in apical (AP), basolateral (BL), and intracellular (Cell) compartments at the end of the study, t is the

DMD Fast Forward. Published on August 22, 2018 as DOI: 10.1124/dmd.118.083246
This article has not been copyedited and formatted. The final version may differ from this version.

reaction time (120 min), and $C_{0,\,PD(AP)}$ is the initial concentration of test prodrugs on the apical side.

Subsection 5: Permeation Experiment of 14 Drugs across hiPSC-IEC Monolayers for Comparison of P_{app} values with Human Fa. The apical to basolateral permeabilities of 14 drugs (ganciclovir, doxorubicin, sulfasalazine, [^{14}C]mannitol, sulpiride, famotidine, ranitidine, atenolol, furosemide, hydrochlorothiazide, [^{3}H]digoxin, acetaminophen, propranolol, and antipyrine) were measured under the same conditions as described in Subsection 2 except for sampling times. Test concentrations of ganciclovir, doxorubicin, [^{14}C]mannitol, sulfasalazine, and [^{3}H]digoxin were set at 100 μM, 2 μM, 10 μM (20 μCi/mL), 2 μM, and 1 μM (1 μCi/mL), respectively, and the test concentration of the other nine drugs (famotidine, sulpiride, atenolol, furosemide, ranitidine, hydrochlorothiazide, acetaminophen, propranolol, and antipyrine) was set at 10 μM. For propranolol and antipyrine transport studies, sampling times were set at 30, 60, and 90 min, and for the other 12 compound transport studies, sampling times were set at 1, 2, and 3 hr.

In transcellular transport assessment using Caco-2 cells, the K_m values of doxorubicin, digoxin for P-gp, and sulfasalazine for BCRP were reported to be >100 μM, 177 μM, and 369 μM, respectively (Liang et al., 2000; Troutman and Thakker, 2003; Kim et al., 2013). The concentrations of these drugs in the present study are well below their reported K_m values, assuming that these transporters are not saturated.

When the drug migration in the gastrointestinal tract is assumed to follow a well-stirred model according to the previous report (Amidon et al., 1988), the following equations are obtained:

$$C_{out}/C_{in} = e^{\{ - (S/V) \times P_{app} \times t_{res}\}} \quad \text{(Eq. 5)}$$

$$C_{out}/C_{in} = 1 - Fa \quad \text{(Eq. 6)}$$

$$Fa = 1 - e^{\{ - (S/V) \times P_{app} \times t_{res}\}} = e^{-SF \times P_{app}} \quad \text{(Eq. 7)}$$

$$(SF = (S/V) \times t_{res})$$

where C_{in} and C_{out} represent the drug concentration of the inlet and outlet of the gastrointestinal tract, respectively. S and V represent the surface area and volume of the gastrointestinal tract per unit length of the small intestine, respectively. t_{res} represents the average residence time of drugs in small intestine. P_{app} represents the permeability coefficient of intestinal epithelial cells and can be estimated by transcellular transport study across hiPSC-IEC monolayers. Since S, V, and t_{res} are treated as fixed values, SF (the empirical scaling factor) can be obtained by the fitting study between P_{app} in hiPSC-IECs and human Fa of 14 drugs using a nonlinear least-square method by XLfit software (ID Business Solution, Guildford, UK).

Pharmacokinetic Studies of Six Ester Prodrugs in Rats. For oral administration studies of six ester prodrugs, each was suspended in an aqueous solution of 0.5% (w/v) methylcellulose 400 cP at a concentration of 1 mg/5 mL/kg as its active form and orally administrated to rats (n = 2 or 3). Rats had been anesthetized with isoflurane and catheterized into the jugular vein for subsequent blood sampling 3 days before the experiment. Blood samples were collected from the jugular vein with a

heparinized syringe 0.25, 0.5, 1, 2, 4, 6, 8, and 24 hr after administration.

For intravenous administration studies of the active form, this form was dissolved in dimethyl acetamide and propylene glycol solution (1:1, v/v) at a concentration of 1 mg/1 mL/kg, and administered via the caudal vein to rats (n = 3). Blood samples were collected from the jugular vein with a heparinized syringe 0.033, 0.083, 0.25, 0.5, 1, 2, 4, 6, 8, and 24 hr after administration.

The collected blood samples were centrifuged at 1,310 × g for 10 min at 4°C and the resulting supernatants were collected as plasma samples. The pharmacokinetic parameters for the plasma concentration of the active form were calculated via non-compartmental analysis by using WinNonlin 5.0 software (Pharsight, Mountain View, CA) with uniform weighting. The C_{max} (ng/mL) was the maximum concentration among the sampling times (0.25, 0.5, 1, 2, 4, 6, 8, and 24 hr after oral administration). The AUC (ng × hr/mL) was calculated by the linear trapezoidal method. BA (%) was calculated using the following equation:

$$BA = \frac{AUC_{p.o.} / Dose_{p.o.}}{AUC_{i.v.} / Dose_{i.v.}} \times 100 \quad \text{(Eq. 8)}$$

where $AUC_{p.o.}$ and $Dose_{p.o.}$ represent AUC (ng × hr/mL) of the active form and the dose of prodrugs (1 mg/kg as the active form) for oral administration of prodrugs, respectively. $AUC_{i.v.}$ and $Dose_{i.v.}$ represent AUC (ng × hr/mL) of the active form and dose (1 mg/kg) for intravenous administration of the active form, respectively.

Measuring Radioactivity Using a Liquid Scintillation Counter. Samples of

radiolabeled compounds, [^{14}C]mannitol, [^{3}H]digoxin, and [^{14}C]glycylsarcosine, were mixed with Pico-Fluor Plus (PerkinElmer, Waltham, MA). The radioactivity levels were measured using a liquid scintillation counter (Tri-Carb 3100TR; PerkinElmer).

Quantification of Test Compounds Using LC-MS/MS. The concentrations of test compounds except for radiolabeled compounds were quantified using LC-MS/MS. The samples were stored at -20°C until determination of the compounds. For the transcellular transport studies in hiPSC-IECs and Caco-2 cells, a 6-fold volume of acetonitrile was added to the samples, whereas for the pharmacokinetics studies in rat, a 12.5-fold volume of acetonitrile was added to samples. The samples were centrifuged at 1,880 × g for 5 min at 4°C, and then the resulting supernatants were injected into the LC-MS/MS system. The measurement condition using LC-MS/MS were developed in Shionogi & Co., Ltd. The detailed LC-MS/MS conditions are shown in Table S4. Chromatogram ion counts were determined by using Analyst software version 1.6 (AB SCIEX) or MassLynx software version 4.1 (Waters, Milford, MA).

For the quantifications of test compounds using LC-MS/MS, a calibration curve was prepared using a dilution series of each compound. The concentrations of calibration standards are back-calculated, and the difference between the back-calculated concentration of the calibration standard and its nominal concentration was determined. The present study accepted the range of calibration standards if the difference between the back-calculated concentration of the calibration standard and its nominal concentration is within ± 15%, and the lowest concentration in the calibration standard was defined as a limit of quantification.

DMD Fast Forward. Published on August 22, 2018 as DOI: 10.1124/dmd.118.083246
This article has not been copyedited and formatted. The final version may differ from this version.

Statistical Analysis. The statistical significance of differences between two groups was determined by Student's t-test. A value of $p < 0.05$ was considered statistically significant.

DMD Fast Forward. Published on August 22, 2018 as DOI: 10.1124/dmd.118.083246
This article has not been copyedited and formatted. The final version may differ from this version.

Results

Generation of hiPSC-IECs. Differentiation from hiPSCs to human intestinal epithelial cells was verified by determining the differentiation markers for hiPSCs, definitive endoderms (DEs), hindguts (HGs), and intestinal epithelial cells according to the differentiation methods described in Supplemental Data. In the differentiated DEs, the gene expression levels of DE markers, SOX17, FOXA2, and GATA4, were markedly higher in DEs than those in hiPSCs (Fig. S2A). Immunofluorescence analysis also showed that the protein expression of SOX17 was detected in DEs but not in hiPSCs (Fig. S2B). The differentiated HGs dramatically increased the gene expression level of HG marker (CDX2) compared with that in hiPSCs and DEs (Fig. S2A). The protein expression of CDX2 was also detected in HGs but not in hiPSCs and DEs by immunofluorescence analysis (Fig. S2B). Furthermore, undifferentiated markers (OCT3/4 and SOX2) gradually decreased in the process of differentiations of DEs and HGs (Fig. S2A). When hiPSC-IECs isolated from intestinal organoids by means of the magnetic activated cell sorting (MACS) technique were cultured on Transwell insert for 21 days, the gene expressions of the enterocyte markers (LGR5 and ISX), the intestinal epithelial markers (VIL and SI), the paneth cell marker (LYZ), the endocrine cell marker (CHGA), and the goblet cell markers (MUC2 and TFF3) increased compared to those in hiPSCs (Fig. S3).

Gene Expression of Transporters and Metabolic Enzymes in hiPSC-IECs, iPSCs, Caco-2 Cells, Adult Small Intestine, and Fetal Small Intestine. The gene expression levels of transporters (P-gp, BCRP, and PEPT1) and metabolic enzymes (CYP3A4, CYP3A7, CES1, CES2, and UGT1A1) in hiPSC-IECs 21 days after

cultivation on Transwell inserts (day 21) were compared with adult and fetal small intestine, Caco-2 cells, hiPSCs, and hiPSC-IECs before cultivation on Transwell inserts (day 0) (Fig. 1).

Comparing the gene expression between day 0 and day 21 of hiPSC-IECs showed higher expression levels at day 21 than at day 0 for P-gp, BCRP, PEPT1, CYP3A4, CES2, and UGT1A1 (5.13-, 16.7-, 2.08-, 5.06-, 1.70-, and 3.29-fold, higher at day 21 than day 0, respectively), although there were no significant differences for PEPT1 and CYP3A4 expression between day 0 and day 21. In contrast, molecules showing lower expression levels at 21 day than at 0 day were CYP3A7 and CES1 (3.87- and 7.38-fold, lower at day 21 than day 0, respectively). For the comparison of expression between hiPSC-IECs of 21-day cultivation and adult small intestine, P-gp, BCRP, PEPT1, CYP3A4, CES1, CES2, and UGT1A1 in hiPSC-IECs were expressed at 11.1-, 11.6-, 4.59-, 274-, 336-, 16.4-, and 4.46-fold lower levels than those in adult small intestine, respectively. Comparing expression between hiPSC-IECs of 21-day cultivation and Caco-2 cells, P-gp, BCRP, PEPT1, and CES1 expressions were 4.55-, 3.76-, 1.02-, 7580-fold, respectively, lower in hiPSC-IECs than in Caco-2 cells, whereas CYP3A4, CYP3A7, CES2, and UGT1A1 expressions were 30.6-, 18.8-, 1.33-, 16.9-fold, respectively, higher in hiPSC-IECs than in Caco-2 cells.

Formation of Tight Junction in hiPSC-IEC and Caco-2 Cell Monolayers. The TEER value and the permeability of [^{14}C]mannitol, a paracellular marker, was examined to evaluate the tight junction formation in hiPSC-IEC monolayers. The TEER value in hiPSC-IEC monolayers on 24 well Transwell inserts was recorded every 1-3 day until 21 days after seeding on Transwell inserts. The TEER values in hiPSC-IEC

DMD Fast Forward. Published on August 22, 2018 as DOI: 10.1124/dmd.118.083246
This article has not been copyedited and formatted. The final version may differ from this version.

monolayers increased in a time-dependent manner and reached 329 ± 20 ($\Omega \times cm^2$) 21 days after seeding on Transwell inserts (Fig. 2A). In contrast, the TEER values in Caco-2 cell monolayers were 891 ± 26 ($\Omega \times cm^2$) 21 days after seeding on Transwell inserts, which were significantly higher than those in hiPEC monolayers. The P_{app} values of [^{14}C]mannitol in hiPSC-IEC and Caco-2 cell monolayers 21 days after seeding on Transwell inserts were 0.222 ± 0.020 ($\times 10^{-6}$ cm/sec) and 0.167 ± 0.007 ($\times 10^{-6}$ cm/sec), respectively (Fig. 2B). There was no significant difference of the P_{app} values of [^{14}C]mannitol between hiPSC-IECs and Caco-2 cells. These results suggested that hiPSC-IECs formed tight junctions. Detail discussion for formation of tight junction in hiPSC-IECs is described in the Supplemental Data.

Functional Expression of P-gp and BCRP in hiPSC-IEC Monolayers. The bi-directional (apical-to-basolateral and basolateral-to-apical) transcellular transport studies across hiPSC-IEC monolayers were performed to investigate the function of P-gp and BCRP in hiPSC-IECs. The P_{app} values of [^{3}H]digoxin (a P-gp substrate) in the basolateral-to-apical direction were significantly higher than that in apical-to-basolateral direction (efflux ratio, 2.43 ± 0.18), and the efflux ratio decreased to 0.743 ± 0.083 by 10 μM cyclosporin A (a P-gp inhibitor) (Fig. 3A). Also, the P_{app} values of sulfasalazine (a BCRP substrate) in the basolateral-to-apical direction were significantly higher than that in the apical-to-basolateral direction (efflux ratio, 3.65 ± 0.49), and the efflux ratio decreased to 1.16 ± 0.33 by 0.1 μM KO143 (a BCRP inhibitor) (Fig. 3B). The membrane localizations of P-gp and BCRP in hiPSC-IECs were not measured by immunofluorescence confocal microscopy. However, the functional analysis of the P-gp and BCRP indicate that P-gp and BCRP expressed in the apical membrane of

hiPSC-IECs. Detail discussion for membrane localizations of P-gp and BCRP in hiPSC-IECs is described in the Supplemental Data.

Functional Expression of PEPT1 in hiPSC-IEC Monolayers. The apical-to-basolateral transport activity across hiPSC-IEC monolayers was measured to investigate the function of PEPT1 in hiPSC-IECs. The P_{app} value of 10 μM [^{14}C]glycylsarcosine (a PEPT1 substrate) was 7.90 ± 0.31 ($\times 10^{-6}$ cm/sec) and decreased to 1.56 ± 0.17 ($\times 10^{-6}$ cm/sec) in the presence of a high concentration (10 mM) unlabeled glycylsarcosine (Fig. 3C). The result of functional analysis in the transcellular transport study indicates that PEPT1 expressed in the apical membrane of hiPSC-IECs. Detail discussion for membrane localizations of PEPT1 in hiPSC-IECs is described in the Supplemental Data.

Functional Expression of CYP3A4, CES2 and CES1 in hiPSC-IEC Monolayers. The metabolic activities of CYP3A4, CES2, and CES1 in iPSC-IECs and Caco-2 cells were determined by the extraction ratio calculated by using Eq. 3. The extraction ratio of metabolism of midazolam (a substrate of CYP3A4) to 1-OH midazolam in hiPSC-IECs was 0.534 ± 0.009 (%), and decreased to 0.322 ± 0.009 (%), and 0.0821 ± 0.0064 (%) in the presence of 0.5 μM and 10 μM ketoconazole (an inhibitor of CYP3A4), respectively (Fig. 4A). The extraction ratio in Caco-2 cells was 0.0623 ± 0.0038 (%) and also decreased to 0.0404 ± 0.0023 (%), and 0.0414 ± 0.0032 (%) in the presence of 0.5 μM and 10 μM ketoconazole, respectively (Fig. 4A).

The extraction ratio of metabolism of irinotecan (a CES2 substrate) to SN38 in hiPSC-IECs was 3.52 ± 0.15 (%), and decreased to 2.42 ± 0.17 (%) in the presence of

DMD Fast Forward. Published on August 22, 2018 as DOI: 10.1124/dmd.118.083246
This article has not been copyedited and formatted. The final version may differ from this version.

100 μM telmisartan (a CES2 inhibitor) (Fig. 4B). The extraction ratio in Caco-2 cells was 3.96 ± 0.55 (%), and also decreased to 2.30 ± 0.30 (%) in the presence of 100 μM telmisartan (Fig. 4B). SN38 is glucuronidated to SN38 glucuronide by UGT1A1 (Hanioka et al., 2001). However, the positive chromatogram peak of SN38 glucuronide by LS-MS/MS analysis was not detected in all samples of metabolic assessment of irinotecan in hiPSC-IECs and Caco-2 cells (data was not shown).

The extraction ratio value of metabolism of temocapril (a CES1 substrate) to temocaprilat in the absence and presence of 500 μM BNPP (a CES inhibitor) in hiPSC-IECs were 4.17 ± 0.22 (%) and 5.18 ± 0.30 (%), respectively (Fig. 4C). In contrast, the extraction ratio in Caco-2 cells was 99.0 ± 0.1 (%) and decreased to 1.29 ± 0.07 (%) in the presence of 500 μM BNPP (Fig. 4C).

Comparison of Hydrolysis Activity of Six Prodrugs between hiPSC-IEC Monolayers and Pharmacokinetic Parameters in Rats. The hydrolysis activities of six ester prodrugs (prodrugs A, B, C, D, E, and F) to a common active form in hiPSC-IEC monolayers were assessed by CL_{int} determined using Eq. 4. The values of C_{max}, AUC, and BA of the six prodrugs in SD rat were calculated from the plasma concentrations of the active form after oral administrations of the six prodrugs. As shown in Fig. 5 and Table S5, the CL_{int} values of the six prodrugs in hiPSC-IEC monolayers were correlated with C_{max}, AUC, and BA in SD rat (correlation coefficients were 0.840, 0815, and 0.815, respectively).

Comparison of the P_{app} Values of 14 Drugs across hiPSC-IEC Monolayers with Their Fa Values in Humans. To examine whether Fa values in humans can be

DMD Fast Forward. Published on August 22, 2018 as DOI: 10.1124/dmd.118.083246
This article has not been copyedited and formatted. The final version may differ from this version.

predicted from the values of P_{app} across iPSC-IEC monolayers, the P_{app} values of 14 compounds (ganciclovir, doxorubicin, [^{14}C]mannitol, famotidine, sulpiride, atenolol, sulfasalazine, furosemide, ranitidine, hydrochlorothiazide, [^{3}H]digoxin, acetaminophen, propranolol, and antipyrine) across iPSC-IECs were comparted with their human Fa values taken from previous reports (Zhao et al., 2001; Sugano et al., 2002; Varma et al., 2010). If multiple Fa values are reported in these literatures, the median value was calculated and used (Table S6). As shown in Fig. 6, the P_{app} values of 14 compounds in iPSC-IECs were correlated well with human Fa values (Fig. 6 and Table S6).

The value of SF of Eq. 7 was calculated as 2.96 from the correlation plot between the values of P_{app} in hiPSC-IECs and human Fa of 14 drugs. Hence, the following equation for prediction of human Fa values from the P_{app} values in hiPSC-IECs can be obtained:

$$Fa = e^{-2.96 \times P_{app}} \quad \text{(Eq. 9)}$$

As a result of the regression statistics between the predicted values of human Fa on the basis of the above equation and the observed ones of 14 drugs, the determination coefficient was calculated to be 0.691. For 12 compounds except for [^{14}C]mannitol and ranitidine, the predicted human Fa values showed within 3-fold differences comparted to observed ones (Table S6).

DMD Fast Forward. Published on August 22, 2018 as DOI: 10.1124/dmd.118.083246
This article has not been copyedited and formatted. The final version may differ from this version.

Discussion

Many researchers have succeeded in generating hiPSC-IECs showing functions of intestinal transporters and metabolic enzymes (Spence et al., 2011; Kauffman et al., 2013; Ogaki et al., 2013; Forbester et al., 2015; Iwao et al., 2015; Ozawa et al., 2015; Uchida et al., 2017). However, whether these functions in oral drug absorption can be predicted using hiPSC-IECs remained to be clarified. This study is the first to demonstrate that the hydrolysis of six ester prodrugs into the active form in hiPSC-IECs was correlated with the plasma exposures of the active form after oral administration of these prodrugs in rats. Furthermore, the P_{app} values of 14 drugs, containing substrates of P-gp and BCRP, were correlated with their human Fa values.

P-gp, BCRP, and PEPT1 play important roles in intestinal drug absorption. The functions of BCRP and PEPT1 in hiPSC-IECs have been previously reported (Iwao et al., 2015; Ogaki et al., 2015; Ozawa et al., 2015; Kodama et al., 2016; Uchida et al., 2017), while the present study was the first to reveal the functional expression of P-gp in hiPSC-IECs. The P_{app} value of [^{3}H]digoxin (a P-gp substrate) in the basolateral-to-apical direction was greater than that in the apical-to-basolateral one (efflux ratio, 2.43), and the differences of P_{app} in these two directions disappeared in the presence of cyclosporin A (efflux ratio, 0.743) (Fig. 3A). The efflux ratio of digoxin in human jejunum based on the Ussing chamber technique was reported to be 5.41 (Sjoberg et al., 2013), and the value was 2.25-fold higher compared to the present study. We found 11.1-fold lower gene expression of P-gp in hiPSC-IECs than that in adult human small intestine (Fig. 1), supporting the difference of P-gp activity between hiPSC-IECs and human jejunum. Besides P-gp, the efflux transport of sulfasalazine (a BCRP substrate) and influx transport of [^{14}C]glycylsarcosine (a PEPT1 substrate) were

reduced by inhibitors of BCRP and PEPT1, indicating that hiPSC-IECs have the transport activities of BCRP and PEPT1 (Figs. 3B and 3C). These results showed that hiPSC-IECs can be used to investigate drug absorption of the substrates of P-gp, BCRP, and PEPT1, although gene expression levels of these transporters in hiPSC-IECs were lower than those in adult intestine (Fig. 1).

CYP3A contributes to the intestinal first-pass metabolism. Study of CYP3A4 activity in hiPSC-IECs showed that midazolam was metabolized to 1-OH midazolam, and the metabolizing activity of CYP3A4 was higher in hiPSC-IECs than in Caco-2 cells (Fig. 4A). This reflects the difference in the gene expression of CYP3A4 between hiPSC-IECs and Caco-2 cells (Fig. 1). Since the gene expression level of CYP3A4 was 274-fold lower in hiPSC-IECs than in human small intestine (Fig. 1), the metabolic activity of CYP3A4 in hiPSC-IECs was surmised to be lower than in human small intestine.

In this study, hiPSC-IECs showed lower expression of transporters and metabolic enzymes than human small intestine. A previous report suggested that hiPSC-IECs more closely resemble fetal rather than adult intestine by unsupervised hierarchical clustering of RNA-sequencing data (Finkbeiner et al., 2015). Miki et al. demonstrated that P-gp and CYP3A4 were more highly expressed in adult than fetal intestine (Miki et al., 2005). Taken together, hiPSC-IECs represent immature characteristics. We showed that the gene expression level of CYP3A4 in hiPSC-IECs cultured on Transwell filter for 21 days tended to be higher than that before cultivation on Transwell filter, whereas the expression of CYP3A7, a predominant CYP3A isoform in fetal human small intestine (Shin et al., 2009; Betts et al., 2015), in hiPSC-IECs decreased when cultivated on Transwell filter (Fig. 1). This expression pattern might

imply the development of hiPSC-IECs from fetal to adult form. Since the expressions of transporters and metabolic enzymes are still low compared to human small intestine, the culture conditions for further enhancing the degree of maturation and expression of transporters and metabolic enzymes in hiPSC-IECs needs to be clarified.

CES is involved in the hydrolysis of ester prodrugs. There are two major isoforms (CES1 and CES2) in humans, and CES2 is highly expressed in small intestine (Hosokawa, 2008). CES1 is more highly expressed than CES2 in Caco-2 cells (Imai et al., 2005). Since there is a difference of substrate specificity between CES2 and CES1 (Hosokawa, 2008), the hydrolysis of ester prodrugs in Caco-2 cells does not reflect that in human small intestine. Imai et al. demonstrated that hydrolysis of temocapril (a substrate of CES1) was not detected in human small intestinal microsomes but detected in the S9 membrane fraction of Caco-2 cells (Imai et al., 2005). Also, Ishiguro et al. proposed that the intestinal absorption of dabigatran etexilate (a substrate of CES1) was misread using Caco-2 cells due to overestimation of the contribution of hydrolysis via CES1 (Ishiguro et al., 2013). In the present study, the expression level of CES2 in hiPSC-IECs was almost equal to that in Caco-2 cells, whereas CES1 was more highly expressed in Caco-2 cells than hiPSC-IECs (Fig. 1). Similarly, the hydrolysis activity of irinotecan (a substrate of CES2) was almost the same as that in Caco-2 cells (Fig. 4B), whereas the hydrolysis activity of temocapril was markedly greater in Caco-2 cells than hiPSC-IECs (Fig. 4C). These results imply that hiPSC-IECs may be a useful model for studying intestinal hydrolysis activity with little influence from CES1 mediated hydrolysis compared to Caco-2 cells.

To examine whether in vivo hydrolysis in small intestine can be investigated using hiPSC-IECs, we compared the hydrolysis of six ester prodrugs in hiPSC-IECs

DMD Fast Forward. Published on August 22, 2018 as DOI: 10.1124/dmd.118.083246
This article has not been copyedited and formatted. The final version may differ from this version.

with C_{max}, AUC, and BA of the active form after oral administration to rats. CL_{int}, a parameter reflecting the hydrolysis rate of a prodrug into its active form, increases as the hydrolysis rate of the prodrug increases. CL_{int} values of the six prodrugs in hiPSC-IECs were correlated well with each pharmacokinetic parameter for rats (Fig. 5 and Table S5). CL_{int} of the prodrugs in hiPSC-IECs reflected two processes: permeation of the prodrug into the cells and hydrolysis of the prodrug to its active form in the cells (Eq. S1 and Fig. S4). Whereas, besides these two processes, intestinal absorption of prodrugs includes permeation from the intestinal cells to the portal vein of the active form produced by hydrolysis of prodrugs (Eq. S2 and Fig. S4). Since the six prodrugs used in the present study were all hydrolyzed into a common active form, the permeability the basolateral efflux of the active form was the same for these prodrugs (Eq. S3). Thus, CL_{int} values can be correlated with the absorption rate of a prodrug in the intestinal lumen and with intestinal hydrolysis based on pharmacokinetic theory. Although we did not confirm species differences of the hydrolysis activities of these six prodrugs between human and rat small intestine, CL_{int} of prodrugs in hiPSC-IECs might be useful as an index for in vivo hydrolysis activities in prodrugs derived from a common active form. Further study is needed to clarify whether hydrolysis of prodrugs in hiPSC-IECs also reflects that in human intestine.

Since hiPSC-IECs formed tight junctions and have the function of drug transporters, we compared the P_{app} values of 14 drugs in hiPSC-IECs with their human Fa values. These 14 drugs included two P-gp substrates, one BCRP substrate, and 11 non-substrates of transporters. The P_{app} values of the 14 drugs in hiPEC-IECs were correlated with their human Fa values (Fig.6 and Table S6). This suggested that hiPSC-IECs could predict the oral absorption of drugs in human small intestine by

various mechanisms, such as passive diffusion and efflux transport via P-gp and BCRP. According to the previous report (Amidon et al., 1988), theoretical fitting curve was created between the values of P_{app} in hiPSC-IECs and human Fa of 14 drugs. Since the determination coefficient was high (0.691), it was suggested that the methodology of prediction of human Fa values from P_{app} of hiPSC-IECs was theoretically reasonable. However, predicted human Fa values of [^{14}C]mannitol and ranitidine showed more than 3-fold differences comparted to observed ones (Table S6). There is a possibility of the contribution of transporters to intestinal absorption. However, as a result the parallel artificial membrane permeation assay (PAMPA), which can predict human Fa of drugs via the passive absorption processes, the predicted and observed Fa values of [^{14}C]mannitol and ranitidine were relatively consistent (Sugano et al., 2002). This indicated that there is little contribution of transporters to intestinal absorption of [^{14}C]mannitol and ranitidine. It will be necessary to conduct further studies in order to clarify the reason why these drugs are outlier.

In conclusion, we generated hiPSC-IECs that possess crucial factors in drug oral absorption: tight junctions, transporters (P-gp, BCRP, and PEPT1) and metabolic enzyme (CYP3A4, CES2, and CES1). The hydrolysis activities of six ester prodrugs into the active form in hiPSC-IECs were correlated with the plasma exposures of the active form after oral administration of these prodrugs in rat. Furthermore, the permeability coefficients of 14 drugs in hiPSC-IECs were also correlated with human Fa values. Therefore, hiPSC-IECs should be a useful cell model for studying drug absorption in the small intestine. For drugs metabolized in the small intestine, it is important to predict not only Fa but also the fraction escaping intestinal extraction (Fg). Since the expression of CYP3A4 was much lower in hiPSC-IECs than human small

DMD Fast Forward. Published on August 22, 2018 as DOI: 10.1124/dmd.118.083246
This article has not been copyedited and formatted. The final version may differ from this version.

intestine, substrates of CYP3A4 were not used for the prediction of the absorption in vivo. If this expression level of CYP3A4 is increased in the future study, it could be expected to calculate the values of Fa × Fg in order to accurately predict the oral absorption of the substrates for transporters and/or metabolic enzymes using hiPSC-IECs.

DMD Fast Forward. Published on August 22, 2018 as DOI: 10.1124/dmd.118.083246
This article has not been copyedited and formatted. The final version may differ from this version.

Acknowledgments

We thank Ms. Maki Minaguchi and Ms. Sayori Nishio (Shionogi Techno Advance Research Co., Ltd., Toyonaka, Japan) for support with the cultivation of hiPSCs and hiPSC-IECs. We also thank Ms. Miho Tachibana and Ms. Tomoka Soda (Shionogi Techno Advance Research Co., Ltd.) for support with quantifying the concentrations of compounds using LC-MS/MS.

Authorship Contributions

Participated in research design: Akazawa, Yoshida, Kawai.

Conducted experiments: Akazawa.

Contributed new reagents or analytic tools: Kawai

Performed data analysis: Akazawa.

Wrote or contributed to the writing of the manuscript: Akazawa, Ohnishi, Kanazu, Takahashi.

References

Akazawa T, Uchida Y, Miyauchi E, Tachikawa M, Ohtsuki S and Terasaki T (2018) High Expression of UGT1A1/1A6 in Monkey Small Intestine: Comparison of Protein Expression Levels of Cytochromes P450, UDP-Glucuronosyltransferases, and Transporters in Small Intestine of Cynomolgus Monkey and Human. *Mol Pharm* **15:**127-140.

Amidon GL, Sinko PJ and Fleisher D (1988) Estimating human oral fraction dose absorbed: a correlation using rat intestinal membrane permeability for passive and carrier-mediated compounds. *Pharm Res* **5:**651-654.

Betts S, Bjorkhem-Bergman L, Rane A and Ekstrom L (2015) Expression of CYP3A4 and CYP3A7 in Human Foetal Tissues and its Correlation with Nuclear Receptors. *Basic Clin Pharmacol Toxicol* **117:**261-266.

Delavenne X, Ollier E, Basset T, Bertoletti L, Accassat S, Garcin A, Laporte S, Zufferey P and Mismetti P (2012) A semi-mechanistic absorption model to evaluate drug-drug interaction with dabigatran: application with clarithromycin. *Br J Clin Pharmacol* **76:**107-113.

Fenner KS, Troutman MD, Kempshall S, Cook JA, Ware JA, Smith DA and Lee CA (2009) Drug-drug interactions mediated through P-glycoprotein: clinical relevance and in vitro-in vivo correlation using digoxin as a probe drug. *Clin Pharmacol Ther* **85:**173-181.

Finkbeiner SR, Hill DR, Altheim CH, Dedhia PH, Taylor MJ, Tsai YH, Chin AM, Mahe MM, Watson CL, Freeman JJ, Nattiv R, Thomson M, Klein OD, Shroyer NF, Helmrath MA, Teitelbaum DH, Dempsey PJ and Spence JR (2015) Transcriptome-wide Analysis Reveals Hallmarks of Human Intestine

Development and Maturation In Vitro and In Vivo. *Stem Cell Reports*.

Fisher JM, Wrighton SA, Watkins PB, Schmiedlin-Ren P, Calamia JC, Shen DD, Kunze KL and Thummel KE (1999) First-pass midazolam metabolism catalyzed by 1alpha,25-dihydroxy vitamin D3-modified Caco-2 cell monolayers. *J Pharmacol Exp Ther* **289:**1134-1142.

Forbester JL, Goulding D, Vallier L, Hannan N, Hale C, Pickard D, Mukhopadhyay S and Dougan G (2015) Interaction of Salmonella enterica Serovar Typhimurium with Intestinal Organoids Derived from Human Induced Pluripotent Stem Cells. *Infect Immun* **83:**2926-2934.

Groer C, Busch D, Patrzyk M, Beyer K, Busemann A, Heidecke CD, Drozdzik M, Siegmund W and Oswald S (2014) Absolute protein quantification of clinically relevant cytochrome P450 enzymes and UDP-glucuronosyltransferases by mass spectrometry-based targeted proteomics. *J Pharm Biomed Anal* **100:**393-401.

Hanioka N, Ozawa S, Jinno H, Ando M, Saito Y and Sawada J (2001) Human liver UDP-glucuronosyltransferase isoforms involved in the glucuronidation of 7-ethyl-10-hydroxycamptothecin. *Xenobiotica* **31:**687-699.

Hosokawa M (2008) Structure and catalytic properties of carboxylesterase isozymes involved in metabolic activation of prodrugs. *Molecules* **13:**412-431.

Humerickhouse R, Lohrbach K, Li L, Bosron WF and Dolan ME (2000) Characterization of CPT-11 hydrolysis by human liver carboxylesterase isoforms hCE-1 and hCE-2. *Cancer Res* **60:**1189-1192.

Imai T, Imoto M, Sakamoto H and Hashimoto M (2005) Identification of esterases expressed in Caco-2 cells and effects of their hydrolyzing activity in predicting human intestinal absorption. *Drug Metab Dispos* **33:**1185-1190.

Ishiguro N, Kishimoto W, Volz A, Ludwig-Schwellinger E, Ebner T and Schaefer O (2013) Impact of endogenous esterase activity on in vitro p-glycoprotein profiling of dabigatran etexilate in Caco-2 monolayers. *Drug Metab Dispos* **42:**250-256.

Iwao T, Kodama N, Kondo Y, Kabeya T, Nakamura K, Horikawa T, Niwa T, Kurose K and Matsunaga T (2015) Generation of enterocyte-like cells with pharmacokinetic functions from human induced pluripotent stem cells using small-molecule compounds. *Drug Metab Dispos* **43:**603-610.

Kabeya T, Matsumura W, Iwao T, Hosokawa M and Matsunaga T (2017) Functional analysis of carboxylesterase in human induced pluripotent stem cell-derived enterocytes. *Biochem Biophys Res Commun* **486:**143-148.

Kauffman AL, Gyurdieva AV, Mabus JR, Ferguson C, Yan Z and Hornby PJ (2013) Alternative functional in vitro models of human intestinal epithelia. *Front Pharmacol* **4:**79.

Keskitalo JE, Zolk O, Fromm MF, Kurkinen KJ, Neuvonen PJ and Niemi M (2009) ABCG2 polymorphism markedly affects the pharmacokinetics of atorvastatin and rosuvastatin. *Clin Pharmacol Ther* **86:**197-203.

Kim JE, Cho HJ, Kim JS, Shim CK, Chung SJ, Oak MH, Yoon IS and Kim DD (2013) The limited intestinal absorption via paracellular pathway is responsible for the low oral bioavailability of doxorubicin. *Xenobiotica* **43:**579-591.

Kodama N, Iwao T, Katano T, Ohta K, Yuasa H and Matsunaga T (2016) Characteristic Analysis of Intestinal Transport in Enterocyte-Like Cells Differentiated from Human Induced Pluripotent Stem Cells. *Drug Metab Dispos* **44:**0.

Kusuhara H, Furuie H, Inano A, Sunagawa A, Yamada S, Wu C, Fukizawa S, Morimoto

N, Ieiri I, Morishita M, Sumita K, Mayahara H, Fujita T, Maeda K and Sugiyama Y (2012) Pharmacokinetic interaction study of sulphasalazine in healthy subjects and the impact of curcumin as an in vivo inhibitor of BCRP. *Br J Pharmacol* **166:**1793-1803.

Liang E, Proudfoot J and Yazdanian M (2000) Mechanisms of transport and structure-permeability relationship of sulfasalazine and its analogs in Caco-2 cell monolayers. *Pharm Res* **17:**1168-1174.

Miki Y, Suzuki T, Tazawa C, Blumberg B and Sasano H (2005) Steroid and xenobiotic receptor (SXR), cytochrome P450 3A4 and multidrug resistance gene 1 in human adult and fetal tissues. *Mol Cell Endocrinol* **231:**75-85.

Miyauchi E, Tachikawa M, Decleves X, Uchida Y, Bouillot JL, Poitou C, Oppert JM, Mouly S, Bergmann JF, Terasaki T, Scherrmann JM and Lloret-Linares C (2016) Quantitative Atlas of Cytochrome P450, UDP-Glucuronosyltransferase, and Transporter Proteins in Jejunum of Morbidly Obese Subjects. *Mol Pharm* **13:**2631-2640.

Ogaki S, Morooka M, Otera K and Kume S (2015) A cost-effective system for differentiation of intestinal epithelium from human induced pluripotent stem cells. *Sci Rep* **5:**17297.

Ogaki S, Shiraki N, Kume K and Kume S (2013) Wnt and Notch signals guide embryonic stem cell differentiation into the intestinal lineages. *Stem Cells* **31:**1086-1096.

Ozawa T, Takayama K, Okamoto R, Negoro R, Sakurai F, Tachibana M, Kawabata K and Mizuguchi H (2015) Generation of enterocyte-like cells from human induced pluripotent stem cells for drug absorption and metabolism studies in

human small intestine. *Sci Rep* **5:**16479.

Paine MF, Hart HL, Ludington SS, Haining RL, Rettie AE and Zeldin DC (2006) The human intestinal cytochrome P450 "pie". *Drug Metab Dispos* **34:**880-886.

Paine MF, Shen DD, Kunze KL, Perkins JD, Marsh CL, McVicar JP, Barr DM, Gillies BS and Thummel KE (1996) First-pass metabolism of midazolam by the human intestine. *Clin Pharmacol Ther* **60:**14-24.

Prueksaritanont T, Gorham LM, Hochman JH, Tran LO and Vyas KP (1996) Comparative studies of drug-metabolizing enzymes in dog, monkey, and human small intestines, and in Caco-2 cells. *Drug Metab Dispos* **24:**634-642.

Rashid TJ, Martin U, Clarke H, Waller DG, Renwick AG and George CF (1995) Factors affecting the absolute bioavailability of nifedipine. *Br J Clin Pharmacol* **40:**51-58.

Rubio-Aliaga I and Daniel H (2008) Peptide transporters and their roles in physiological processes and drug disposition. *Xenobiotica* **38:**1022-1042.

Sato T, Stange DE, Ferrante M, Vries RG, Van Es JH, Van den Brink S, Van Houdt WJ, Pronk A, Van Gorp J, Siersema PD and Clevers H (2011) Long-term expansion of epithelial organoids from human colon, adenoma, adenocarcinoma, and Barrett's epithelium. *Gastroenterology* **141:**1762-1772.

Shin HC, Kim HR, Cho HJ, Yi H, Cho SM, Lee DG, Abd El-Aty AM, Kim JS, Sun D and Amidon GL (2009) Comparative gene expression of intestinal metabolizing enzymes. *Biopharm Drug Dispos* **30:**411-421.

Simpson K and Jarvis B (2000) Fexofenadine: a review of its use in the management of seasonal allergic rhinitis and chronic idiopathic urticaria. *Drugs* **59:**301-321.

Sjoberg A, Lutz M, Tannergren C, Wingolf C, Borde A and Ungell AL (2013)

Comprehensive study on regional human intestinal permeability and prediction of fraction absorbed of drugs using the Ussing chamber technique. *Eur J Pharm Sci* **48:**166-180.

Spence JR, Mayhew CN, Rankin SA, Kuhar MF, Vallance JE, Tolle K, Hoskins EE, Kalinichenko VV, Wells SI, Zorn AM, Shroyer NF and Wells JM (2011) Directed differentiation of human pluripotent stem cells into intestinal tissue in vitro. *Nature* **470:**105-109.

Sugano K, Takata N, Machida M, Saitoh K and Terada K (2002) Prediction of passive intestinal absorption using bio-mimetic artificial membrane permeation assay and the paracellular pathway model. *Int J Pharm* **241:**241-251.

Taipalensuu J, Tornblom H, Lindberg G, Einarsson C, Sjoqvist F, Melhus H, Garberg P, Sjostrom B, Lundgren B and Artursson P (2001) Correlation of gene expression of ten drug efflux proteins of the ATP-binding cassette transporter family in normal human jejunum and in human intestinal epithelial Caco-2 cell monolayers. *J Pharmacol Exp Ther* **299:**164-170.

Takayama N, Nishimura S, Nakamura S, Shimizu T, Ohnishi R, Endo H, Yamaguchi T, Otsu M, Nishimura K, Nakanishi M, Sawaguchi A, Nagai R, Takahashi K, Yamanaka S, Nakauchi H and Eto K (2010) Transient activation of c-MYC expression is critical for efficient platelet generation from human induced pluripotent stem cells. *J Exp Med* **207:**2817-2830.

Tapaninen T, Backman JT, Kurkinen KJ, Neuvonen PJ and Niemi M (2011) Itraconazole, a P-glycoprotein and CYP3A4 inhibitor, markedly raises the plasma concentrations and enhances the renin-inhibiting effect of aliskiren. *J Clin Pharmacol* **51:**359-367.

Troutman MD and Thakker DR (2003) Efflux ratio cannot assess P-glycoprotein-mediated attenuation of absorptive transport: asymmetric effect of P-glycoprotein on absorptive and secretory transport across Caco-2 cell monolayers. *Pharm Res* **20:**1200-1209.

Uchida H, Machida M, Miura T, Kawasaki T, Okazaki T, Sasaki K, Sakamoto S, Ohuchi N, Kasahara M, Umezawa A and Akutsu H (2017) A xenogeneic-free system generating functional human gut organoids from pluripotent stem cells. *JCI Insight* **2:**e86492.

Varma MV, Obach RS, Rotter C, Miller HR, Chang G, Steyn SJ, El-Kattan A and Troutman MD (2010) Physicochemical space for optimum oral bioavailability: contribution of human intestinal absorption and first-pass elimination. *J Med Chem* **53:**1098-1108.

Zhao YH, Le J, Abraham MH, Hersey A, Eddershaw PJ, Luscombe CN, Butina D, Beck G, Sherborne B, Cooper I and Platts JA (2001) Evaluation of human intestinal absorption data and subsequent derivation of a quantitative structure-activity relationship (QSAR) with the Abraham descriptors. *J Pharm Sci* **90:**749-784.

Legend for Figures

Fig. 1. Gene expression levels of metabolic enzymes and transporters in adult small intestine, fetal small intestine, Caco-2 cells, hiPSCs, and hiPSC-IECs. The gene expression levels of metabolic enzymes and transporters in adult small intestine (adult intestine), fetal small intestine (fetal intestine), Caco-2 cells, hiPSCs, and hiPSC-IECs were examined by qPCR analysis as described in Materials and Methods. The total RNAs of adult intestine and fetal intestine were purchased from Clonetech and BioChain Institute Inc., respectively. The total RNAs of Caco-2 cells, hiPSCs, and hiPSC-IECs were isolated using PureLink® RNA Mini Kit. Caco-2 cells were cultured on Transwell insert for 21 days, and hiPSC-IECs were cultured on Transwell inserts for defined periods; day 0 represents the cells before seeding on Transwell insert, and day 7, day 14, and day 21 represent the cells cultured on Transwell insert for 7, 14, and 21 days. The expression level of each gene was normalized by that of GAPDH, and the relative expression ($2^{-\Delta Ct}$) was calculated as described in Materials and Methods. Each data point represents the means (± S.E.M.) of triplicate analyses of a single sample except for CYP3A4 in hiPSCs (n = 2) and CYP3A7 in adult intestine (n = 1). * and $^{\#}$ indicate significant difference of the quantitative value compared with hiPSC-IECs 21 day after seeding on Transwell insert (*$p < 0.05$; $^{\#}p < 0.01$). ‡The gene was not detected.

Fig. 2. TEER values of hiPSC-IEC monolayers (A) and the P_{app} of [^{14}C]mannitol in hiPSC-IEC and Caco-2 cell monolayers (B). (A) HiPSC-IEC monolayers were cultured on 24 well Transwell inserts for 21 days. The TEER values ($\Omega \times cm^2$) of hiPSC-IEC monolayers were determined as the product of the resistance (Ω) and the

surface area of insert (0.33 cm^2). Each data item represents the mean (± S.E.M.) of six independent cells. (B) The P_{app} value of [^{14}C]mannitol (10 μM, 20 μCi/mL) in the apical-to-basolateral direction was measured in hiPSC-IEC and Caco-2 cell monolayers 21 day after seeding on Transwell inserts. Each data item represents the mean (± S.E.M.) of three independent experiments.

Fig. 3. Transcellular transport of [^{3}H]digoxin (A) and sulfasalazine (B), and [^{14}C]glycylsarcosine (C) across hiPSC-IEC monolayers. (A) The P_{app} value of [^{3}H]digoxin (1 μM, 1 μCi/mL) in the apical-to-basolateral (open column) and basolateral-to-apical directions (closed column) across hiPSC-IEC monolayers were measured in the absence (control) and presence of cyclosporin A (10 μM). * and $^{\#}$ indicate significant difference of the P_{app} value in the basolateral-to-apical direction compared with that in the apical-to-basolateral direction (*$p < 0.05$; $^{\#}p < 0.01$). (B) The P_{app} value of sulfasalazine (2 μM) in the apical-to-basolateral (open column) and basolateral-to-apical directions (closed column) across hiPSC-IEC monolayers were measured in the absence (control) and presence of KO143 (0.1 μM). $^{\#}$ indicates significant difference of the P_{app} value in the basolateral-to-apical direction compared with that in the apical-to-basolateral direction ($^{\#}p < 0.01$). (C) The P_{app} value of [^{14}C]glycylsarcosine (10 μM, 0.5 μCi/mL) in the apical-to-basolateral direction across hiPSC-IEC monolayers were measured in the absence (control) and presence of high concentration (10 mM) of unlabeled glycylsarcosine. Each data point represents the mean (± S.E.M.) of three independent experiments. $^{\#}$ indicates significant difference of the P_{app} value in the presence of unlabeled glycylsarcosine compared with that of control ($^{\#}p < 0.01$).

Fig. 4. Metabolism of midazolam (A), irinotecan (B), and temocapril (C) in hiPSC-IEC and Caco-2 cell monolayers. The extraction ratio, a parameter of the contribution of metabolism to permeation across cell monolayers, was determined by means of apical-to-basolateral transcellular transport study in hiPSC-IECs and Caco-2 cells according to the description in Materials and Methods. (A) White, gray, and black columns represent extraction ratio of metabolism of midazolam (2 μM) to 1-OH midazolam in the absence (control) and presence of ketoconazole (0.5 μM and 10 μM) in hiPSC-IECs and Caco-2 cells, respectively. (B) White and gray columns represent extraction ratio of metabolism of irinotecan (100 μM) to SN38 in the absence (control) and presence of telmisartan (100 μM) in hiPSC-IECs and Caco-2 cells, respectively. (C) White and gray columns represent extraction ratio of metabolism of temocapril (100 μM) to temocaprilat in the absence (control) and presence of BNPP (500 μM) in hiPSC-IECs and Caco-2 cells, respectively. Each data represents the mean ± S.E.M. (n = 3). * and $^{\#}$ indicate significant difference of the value of extraction ratio in the presence of inhibitor compared with that of control (*$p < 0.05$; $^{\#}p < 0.01$).

Fig. 5. Comparison of hydrolysis activity of six ester prodrugs in hiPSC-IEC monolayers and pharmacokinetic parameters in rats. CL_{int}, a parameter of hydrolysis activity of ester prodrugs into the active form, was determined by means of the apical-to-basolateral transcellular transport study in hiPSC-IECs as described in Materials and Methods. The CL_{int} values of six ester prodrugs (prodrugs A, B, C, D, E, and F) in hiPSC-IECs were compared with the pharmacokinetic parameters, (A) C_{max}, (B) AUC, and (C) BA, in rats. These pharmacokinetic parameters of six prodrugs in rats

were calculated from the plasma concentrations of the active form after oral administrations of six prodrugs and intravenous administration of the active form. Six ester prodrugs and the active form are in-house compounds synthesized by Shionogi & Co., Ltd., and these six prodrugs are all hydrolyzed into the same active form. Each value of CL_{int} in hiPSC-IECs represents the mean ± S.E.M. of three determinations. Each value of C_{max}, AUC, and BA in rat represents the mean of two or three rats.

Fig. 6. Comparison of P_{app} values of 14 drugs across hiPSC-IEC monolayers with their Fa values in humans. The P_{app} values of 14 drugs was determined by means of the apical-to-basolateral transcellular transport study across hiPSC-IECs. Ganciclovir, doxorubicin, [^{14}C]mannitol, sulfasalazine, and [^{3}H]digoxin were set at concentrations of 100 μM, 2 μM, 10 μM (20 μCi/mL), 2 μM, and 1 μM (1 μCi/mL), respectively, and nine other drugs at 10 μM. The data of doxorubicin represent the mean of duplicate experiments, and the data of 13 other drugs represent the mean ± S.E.M. of triplicate experiments. 1, ganciclovir; 2, doxorubicin; 3, [^{14}C]mannitol; 4, famotidine; 5, sulpiride; 6, atenolol; 7, sulfasalazine; 8, furosemide; 9, ranitidine; 10, hydrochlorothiazide; 11, [^{3}H]digoxin; 12, acetaminophen; 13, propranolol; 14, antipyrine. Circle and triangle symbols represent non-substrate of transporters and substrate of P-gp or BCRP. Human Fa values were taken from the literature (Zhao et al., 2001; Sugano et al., 2002; Varma et al., 2010). If multiple Fa values are reported in these literatures, the median value was calculated and used. The solid line represents the correlation curve between P_{app} values and Human Fa values; $Fa = \exp(-2.96 \times P_{app})$.

Fig. 1

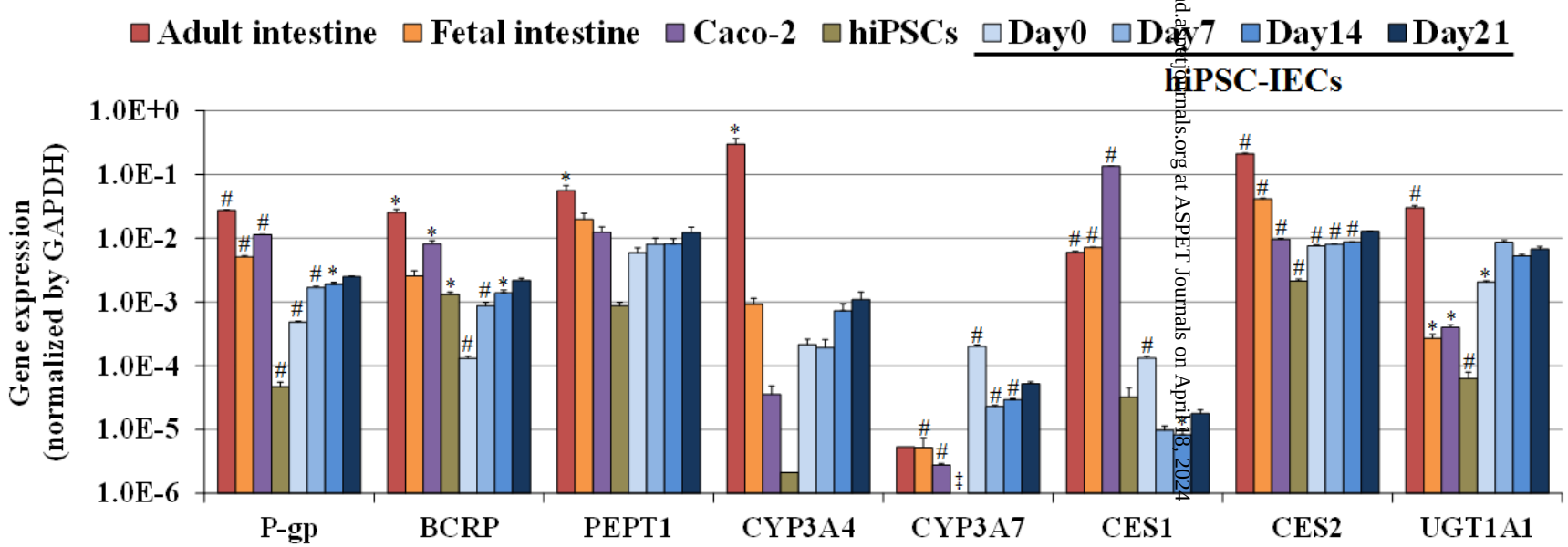

DMD Fast Forward. Published on August 22, 2018 as DOI: 10.1124/dmd.118.083246
This article has not been copyedited and formatted. The final version may differ from this version.

Fig. 2.

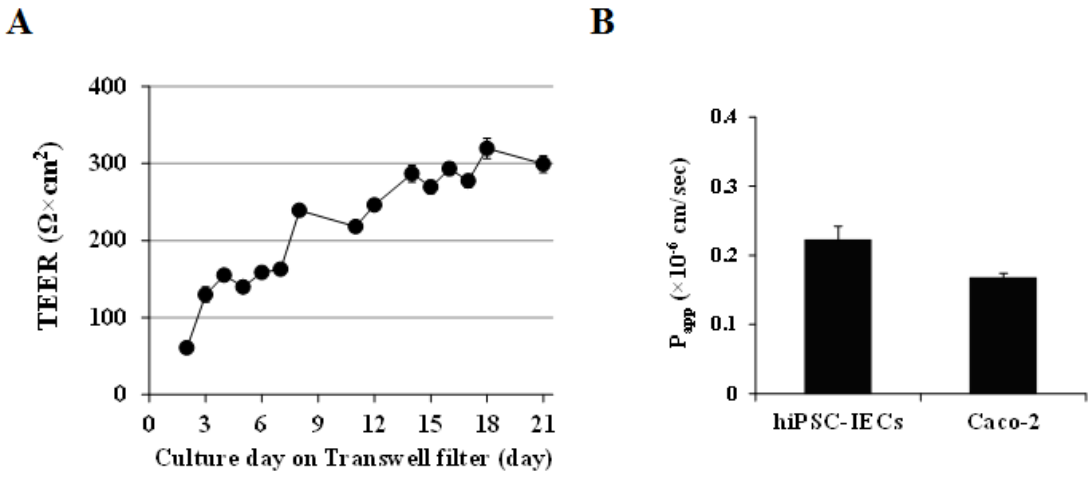

DMD Fast Forward. Published on August 22, 2018 as DOI: 10.1124/dmd.118.083246
This article has not been copyedited and formatted. The final version may differ from this version.

Fig. 3

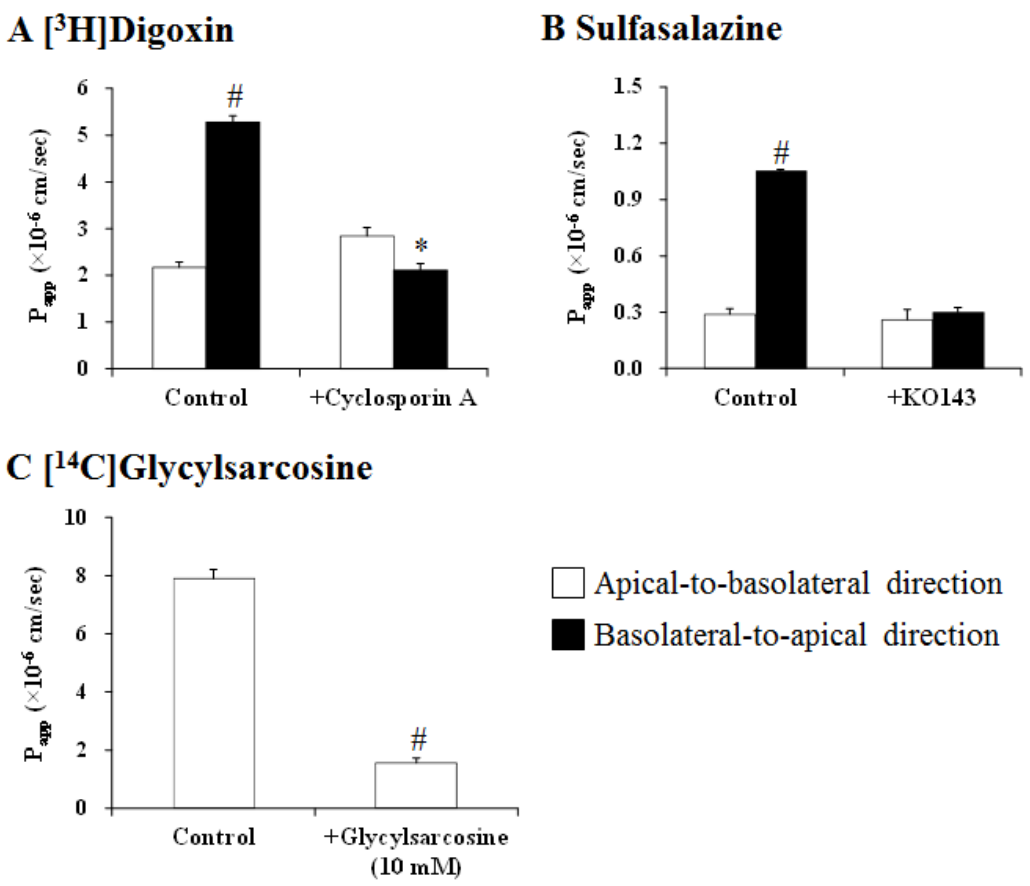

DMD Fast Forward. Published on August 22, 2018 as DOI: 10.1124/dmd.118.083246
This article has not been copyedited and formatted. The final version may differ from this version.

Fig. 4

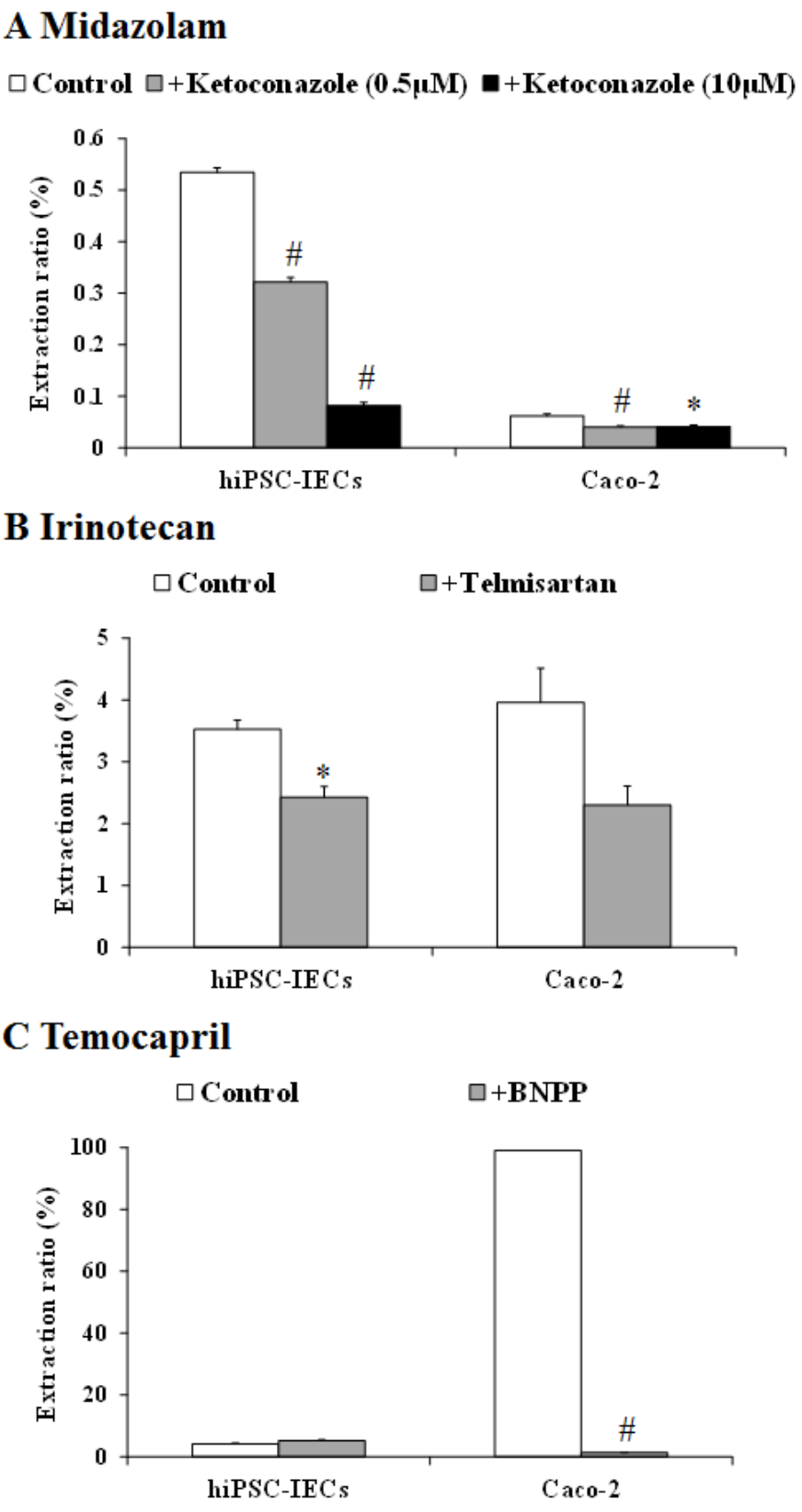

DMD Fast Forward. Published on August 22, 2018 as DOI: 10.1124/dmd.118.083246
This article has not been copyedited and formatted. The final version may differ from this version.

Fig. 5

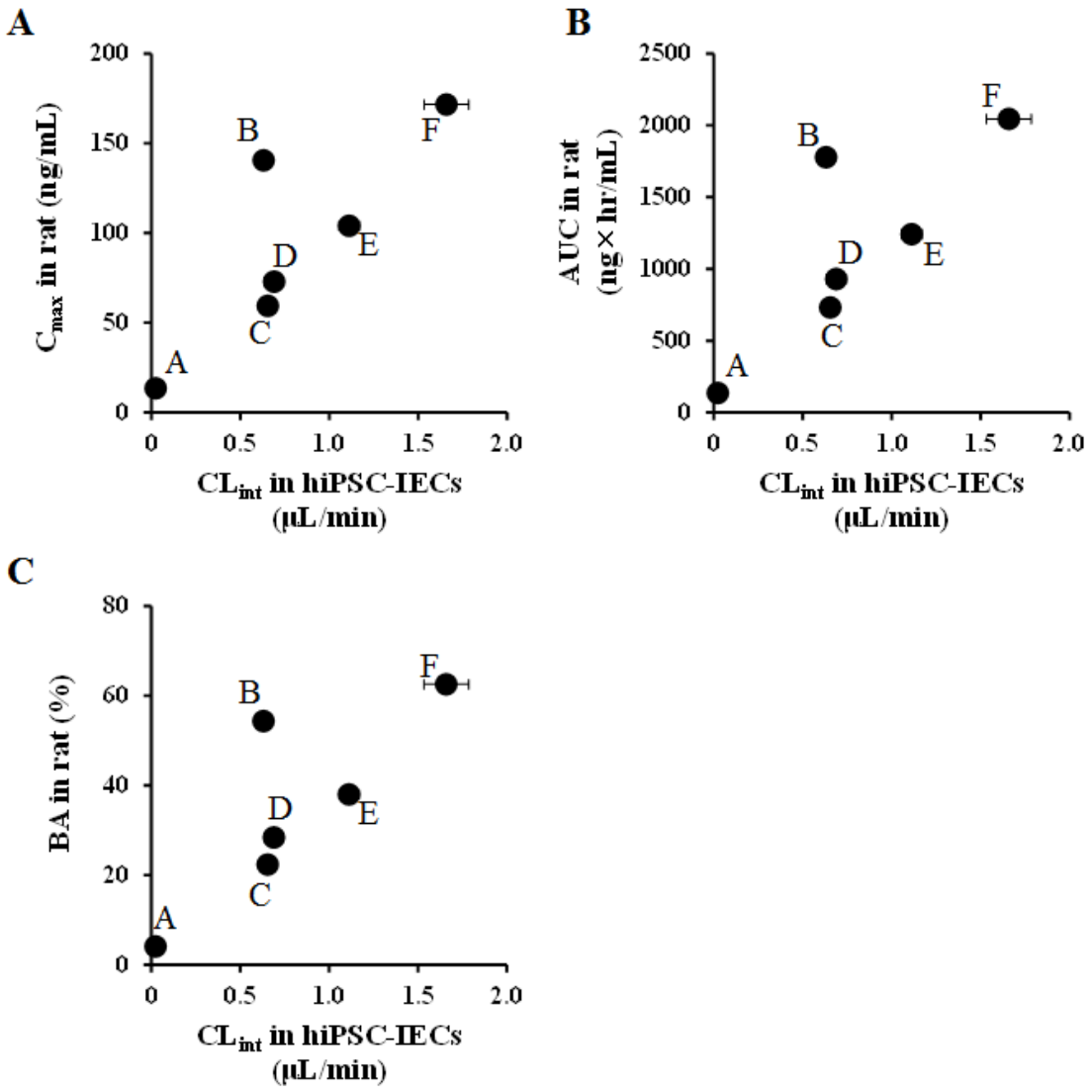

DMD Fast Forward. Published on August 22, 2018 as DOI: 10.1124/dmd.118.083246
This article has not been copyedited and formatted. The final version may differ from this version.

Fig. 6

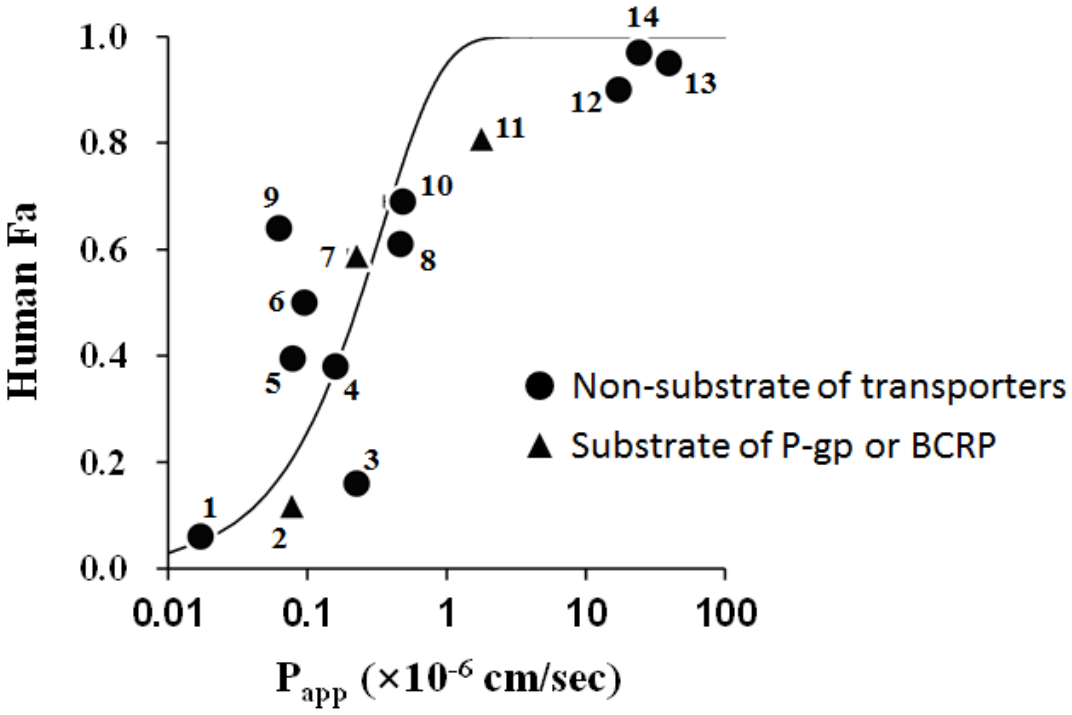

Supplemental Data

Application of Intestinal Epithelial Cells Differentiated from Human Induced Pluripotent Stem Cells for Studies of Prodrug Hydrolysis and Drug Absorption in the Small Intestine

Takanori Akazawa, Shinpei Yoshida, Shuichi Ohnishi, Takushi Kanazu, Makoto Kawai, and Koji Takahashi

Cultivation of hiPSCs. Undifferentiated hiPSCs were maintained on a feeder layer of mitomycin C–treated murine embryonic fibroblasts (MEFs) in hiPSC maintenance medium [DMEM/F-12 (Sigma-Aldrich) supplemented with 20% (v/v) Knockout Serum Replacement (KSR) (Thermo Fisher Scientific), 0.8% (v/v) MEM Non-Essential Amino Acids (NEAA) solution (Thermo Fisher Scientific), 1% (v/v) L-Glutamine–Penicillin–Streptomycin solution (Sigma-Aldrich), 100 μM β-mercaptoethanol (Thermo Fisher Scientific), and 5 ng/mL basic fibroblast growth factor (bFGF; ReproCell, Yokohama, Japan)] at 37°C in humidified atmosphere of 5% CO_2 and 95% air. The medium was changed every day.

Differentiation from hiPSCs into Intestinal Organoids. To generate intestinal organoids, hiPSCs were subjected to stepwise differentiation toward DEs, HGs, and eventual intestinal organoids. The differentiation methods were conducted with minor modifications of the previous report (Spence et al., 2011).

After hiPSCs were pre-incubated with 10 μM Y27632 for 1 hr, feeder cells were removed using dissociation solution (ReproCELL) and colonies of hiPSCs were subsequently dissociated into single cells using accutase (Innovative Cell Tech, San Diego, CA). Dissociated hiPSCs were seeded on 24 well plates (Corning Inc.) coated with Corning Matrigel hESC-Qualified matrix (Corning Inc.) at 3.0×10^5 cells/well, and cultured in hiPSC maintenance medium with 10 μM Y27632 for 24 hr. Next, hiPSCs were cultured for 3 days in DE differentiation medium [RPMI 1640 medium (Thermo Fisher Scientific) supplemented with 100 ng/mL Activin A (R&D systems), 2 mM L-glutamine, 100 units/ml penicillin-streptomycin, and varying concentrations of FBS] to differentiate into DEs. In this culture, the concentrations of FBS were set at 0% on

day 1, 0.2% on day 2, and 2% on day 3. DEs were subsequently cultured for 4 days in HG differentiation medium [RPMI 1640 medium supplemented with 500 ng/ml Wnt3a (R&D systems), 500 ng/ml fibroblast growth factor 4 (FGF4; R&D systems), 2 mM L-glutamine, 100 units/ml penicillin-streptomycin, and 2% FBS] with medium change once daily to obtain HGs. After differentiation into HGs, the whole cells in each well were collected using a cell scraper, and embedded in 55 μl of Corning Matrigel Basement Membrane Matrix (Corning Inc.) containing 500 ng/ml R-Spondin 1, 100 ng/ml Noggin, and 50 ng/ml EGF on Nunclon delta surface tissue culture dishes (Thermo Fisher Scientific). After the Matrigel was solidified at 37°C, the cells were cultured with intestinal differentiation medium [Advanced DMEM/F12 supplemented with 500 ng/ml R-Spondin 1, 100 ng/ml Noggin, 50 ng/ml EGF, 2 mM L-glutamine, 100 units/ml penicillin-streptomycin, 15 mM HEPES, and 2% (v/v) B27 supplement] for 51-69 days to further differentiate into intestinal organoids. In this incubation, the medium was changed every 3 days. All cultures were incubated at 37°C in a humidified atmosphere of 5% CO_2 and 95 % air.

Isolation of Intestinal Epithelial Cells from Intestinal Organoids. Intestinal epithelial cells were isolated by using MACS technique (Miltenyi Biotec, Bergisch Gladbach, Germany) with a magnetic microbeads antibody of CD326 (epithelial cell adhesion molecule; EpCAM), an epithelial cell marker protein. After intestinal organoids were pre-incubated with 10 μM Y27632 for 1 hr, the organoids were washed once with PBS, collected into a tube, and incubated in PBS with 2 mM EDTA (Thermo Fisher Scientific) and 1 mM dithiothreitol (Sigma-Aldrich) for 30 min at 4°C. The suspension was centrifuged at 260 × g for 4 min at room temperature, and the pellet was

suspended and incubated in DMEM/F12 (Thermo Fisher Scientific) with 3 units/ml Dispase II (Roche, Mannheim, Germany), 1% FBS, and 10 μM Y27632 for 20 min at 37°C. The cells were filtrated through a 70 μm cell strainer (Corning Inc.) and centrifuged at 260 × g for 4 min at room temperature. The pellet was suspended in 500 μL of MACS buffer (PBS with 0.1 mM EDTA and 0.5% BSA) containing 2% (v/v) FcR Blocking Reagent (Miltenyi Biotec) and incubated for 10 min at 4°C to avoid non-specific cell labeling. Subsequently, 125 μL of EpCAM MicroBeads (Miltenyi Biotec) was added and the cells were incubated for 15 min at 4°C. After addition of 10 mL of MACS buffer, the suspension was centrifuged at 260 × g for 4 min at room temperature. The obtained pellet was resuspended with MACS buffer, applied onto a MACS column (Miltenyi Biotec) placed in a MACS magnetic holder (Miltenyi Biotec), and 4 mL of MACS buffer was passed through the column three times. Then, the column was removed from a magnetic holder, 5 mL of MACS buffer was added to this column, and EpCAM positive cells were flushed out by firmly pushing the plunger into a tube. After centrifuge at 260 × g for 4 min at room temperature, the resulting pellet was defined as hiPSC-IECs in the present study and suspended with IEC maintenance medium containing 10 μM Y27632. The cell suspension of hiPSC-IECs was subsequently seeded on 24 well Transwell inserts for transcellular transport studies as described in Materials and Methods.

Quantification of Gene Expression of Markers of Undifferentiated Cells, DEs, HGs, and Small Intestine Using qPCR Analysis. Unlike the qPCR for transporters and metabolic enzymes as described in Materials and Methods, qPCR for 15 genes [OCT3/4, SOX2, SOX17, FOXA2, GATA4, CDX2, LGR5, ISX, VIL, SI,

LYZ, CHGA, MUC2, TFF3, and GAPDH (primer 2)] was performed by using an Applied Biosystems 7500 Real Time PCR System using an One Step SYBR® PrimeScript PLUS RT-PCR Kit (Takara Bio Inc., Otsu, Japan), where cDNA synthesis and PCR amplification steps are performed in a single reaction. The reaction solution consisted of 2 μL of RNA, 0.8 μL of 10 μM forward primer (0.4 μM in reaction solution), 0.8 μL of 10 μM reverse primer (0.4 μM in reaction solution), 10 μL of 2 × One Step SYBR® RT-PCR Buffer 4, 0.4 μL of PrimeScript PLUS RTase Mix, 1.2 μL of TaKaRa Ex Taq HS Mix, 0.4 μL of 50 × ROX Reference Dye II, and 4.4 μL of distilled water. The reverse transcription reactions were conducted under the following conditions: 42°C for 5 min, 95°C for 10 sec, followed by 50 cycles of 95°C for 5 sec, 60°C for 34 sec. At the end of each run, a melt curve was generated under the following conditions: 95°C for 15 sec, 60°C for 1 min, and then increasing temperature up to 95°C at 0.5°C increments. The primer information is shown in Table S3. The expression level of each target gene was normalized by that of GAPDH (primer 2). Relative expression of the target gene to GAPDH was calculated using the comparative ΔCt method where ΔCt is obtained by subtracting Ct of GAPDH from the target gene. The relative expression levels of target gene to GAPDH were expressed as $2^{-\Delta Ct}$.

Immunofluorescence Staining. HiPSCs, differentiated DEs and HGs were washed with PBS, and fixed with 4% formaldehyde for 20 min at room temperature. The cells were then washed with PBS and blocked with PBS containing 0.1% Triton-X-100 and 10% normal donkey serum (Jackson Immuno Research Labs., West Grove, PA) for 45 min at room temperature. After washing with PBS, the cells incubated with primary antibodies, 10 μg/mL goat anti-human SOX17 antibody (R&D

Systems, Cat. No. AF1924) or prediluted mouse anti-human CDX2 antibody (BioGenex, San Ramon, CA, Cat. No. AM392), overnight at 4°C. Primary antibodies were removed by washing with PBS, the cells incubated with secondary antibodies, a 1:500 dilution of Alexa Fluor 455-labeled donkey anti-goat antibody (Invitrogen, Cat. No. A-11055) or a 1:500 dilution of Alexa Fluor 455-labeled donkey anti-mouse antibody (Invitrogen, Cat. No. A-31570), for 1 hr at room temperature. Secondary antibodies were removed by washing with PBS, and the cells were incubated with PBS containing Hoechst 33342 (1.62 μM) for 15 min at room temperature. After washing with PBS, PBS was finally added to the cells, and then the fluorescence was measured using a BZ-X710 All-in-One fluorescence microscope (Keyence, Osaka, Japan).

Tight Junction formation in hiPSC-IEC monolayers. An intercellular tight junction barrier restricts permeation through the paracellular pathway in the small intestine. A previous study demonstrated that the P_{app} value of lucifer yellow, a marker for paracellular transport, in Caco-2 cells conspicuously increased when the TEER values were below 200 $\Omega \times cm^2$, but was almost independent of TEER values when they were over 200 $\Omega \times cm^2$ (Hashimoto et al., 1994). This suggested that TEER values exceeding 200 $\Omega \times cm^2$ are needed to study paracellular transport in epithelial cells. The present study showed that the TEER values of hiPSC-IECs increased gradually over time, reaching 299 $\Omega \times cm^2$ at 21 days after seeding on Transwell inserts (Fig. 2A). Also, the P_{app} value of [^{14}C]mannitol, a marker for paracellular transport, in hiPSC-IECs was statistically similar to that of Caco-2 cells showing high TEER values (891 $\Omega \times cm^2$) (Fig. 2B). These results suggested that hiPSC-IECs formed tight junctions strong enough to allow study of paracellular transport.

Membrane localization of the P-gp, BCRP, and PEPT1 in hiPSC-IECs from the Result of Functional Analysis in the Transcellular Transport Study. It is important to examine the membrane localization of the P-gp, BCRP, and PEPT1 for discussing whether hiPSC-IECs can reflect small intestine. In the present study, the membrane localization of P-gp, BCRP, and PEPT1 in hiPSC-IECs was not measured by immunofluorescence confocal microscopy. However, the membrane localization of these transporters can be discussed from the result of functional analysis in the transcellular transport study. P-gp and BCRP play a role for the efflux of substrates from the intracellular-to-extracellular space by driving force of ATP hydrolysis at the intracellular ATP-binding pockets (Higgins and Linton, 2004). PEPT1 transports the substrates from the extracellular-to-intracellular space by the proton gradient (Rubio-Aliaga and Daniel, 2008). As described in Fig. 3, the P_{app} values of [^{3}H]digoxin (a P-gp substrate) and sulfasalazine (a BCRP substrate) in the basolateral-to-apical direction were significantly higher than that in apical-to-basolateral direction, and the transport of [^{14}C]glycylsarcosine was observed in apical-to-basolateral direction (Fig. 3). Therefore, P-gp and BCRP in hiPSC-IECs is consider to mediate the efflux of intracellular-to-apical side, and PEPT1 in hiPSC-IECs is considered to mediate influx of apical-to-intracellular side, indicating that P-gp, BCRP, and PEPT1 could be expressed in the apical membrane of hiPSC-IECs, likewise human small intestine.

Pharmacokinetic Theory for Comparison between CL_{int} Determined Using hiPSC-IECs and Intestinal Absorption Process of Six Ester Prodrugs. The CL_{int} values of six prodrugs in hiPSC-IECs were determined by using (Eq. 4) as described in

Materials and Methods. According the pharmacokinetic model of Fig. S4, CL_{int} could also be expressed by Eq. S1.

$$CL_{int} = PS_{a,\,inf\,(PD)} \times \frac{CL_{hydro\,(PD)}}{PS_{a,\,eff\,(PD)} + PS_{b,\,eff\,(PD)} + CL_{hydro\,(PD)}} \quad \text{(Eq. S1)}$$

where $PS_{a,\,inf\,(PD)}$ (μL/min), $PS_{a,\,eff\,(PD)}$ (μL/min), and $PS_{b,\,eff\,(PD)}$ (μL/min) represent the PS product, the product of the permeability coefficient and the surface area of plasma membrane of per intestinal epithelial cell, for the apical influx, apical efflux, and basolateral efflux of a prodrug, respectively. $CL_{hydro\,(PD)}$ (μL/min) represents the hydrolysis-mediated clearance of a prodrug into its active form in the intestinal epithelial cell.

As shown in Fig. S4, the equation of CL_{int} reflects two processes: permeation of the prodrug into the cells and hydrolysis of the prodrug to its active form in the cells. Whereas, besides these two processes, intestinal absorption of prodrugs includes the process of the basolateral efflux of the active form produced by hydrolysis of prodrugs in the cells. In the present study, we define $CL_{a\,to\,b\,(PD\,to\,AF)}$ (μL/min) as the conversion clearance from a prodrug in the apical side to its active form in the basolateral side via permeation and hydrolysis in intestinal epithelial cells. The equation of $CL_{a\,to\,b\,(PD\,to\,AF)}$ reflects these three processes: the apical influx of a prodrug, hydrolysis of a prodrug into the active form in the cells, and the basolateral efflux of the active form as follows:

$$CL_{a\,to\,b\,(PD\,to\,AF)} = PS_{a,\,inf\,(PD)} \times \frac{CL_{hydro\,(PD)}}{PS_{a,\,eff\,(PD)} + PS_{b,\,eff\,(PD)} + CL_{hydro\,(PD)}} \times \frac{PS_{b,\,eff\,(AF)}}{PS_{a,\,eff\,(AF)} + PS_{b,\,eff\,(AF)}} \quad \text{(Eq. S2)}$$

where $PS_{a,\ eff\ (AF)}$ (μL/min), and $PS_{b,\ eff\ (AF)}$ (μL/min) represent the PS product for the apical efflux and basolateral efflux of the active form, respectively.

Hence, Eq. S2 can be converted to Eq. S3 using Eq. S1.

$$CL_{a\ to\ b\ (PD\ to\ AF)} = CL_{int} \times \frac{PS_{b,\ eff\ (AF)}}{PS_{a,\ eff\ (AF)} + PS_{b,\ eff\ (AF)}} = CL_{int} \times \alpha \quad \text{(Eq. S3)}$$

The value of α reflects the process of the basolateral efflux of the hydrolyzed active form. Since the six prodrugs we investigated were all hydrolyzed into a common active form in the present study, the α value in Eq. S3 is the same for the six prodrugs (Fig. S1).

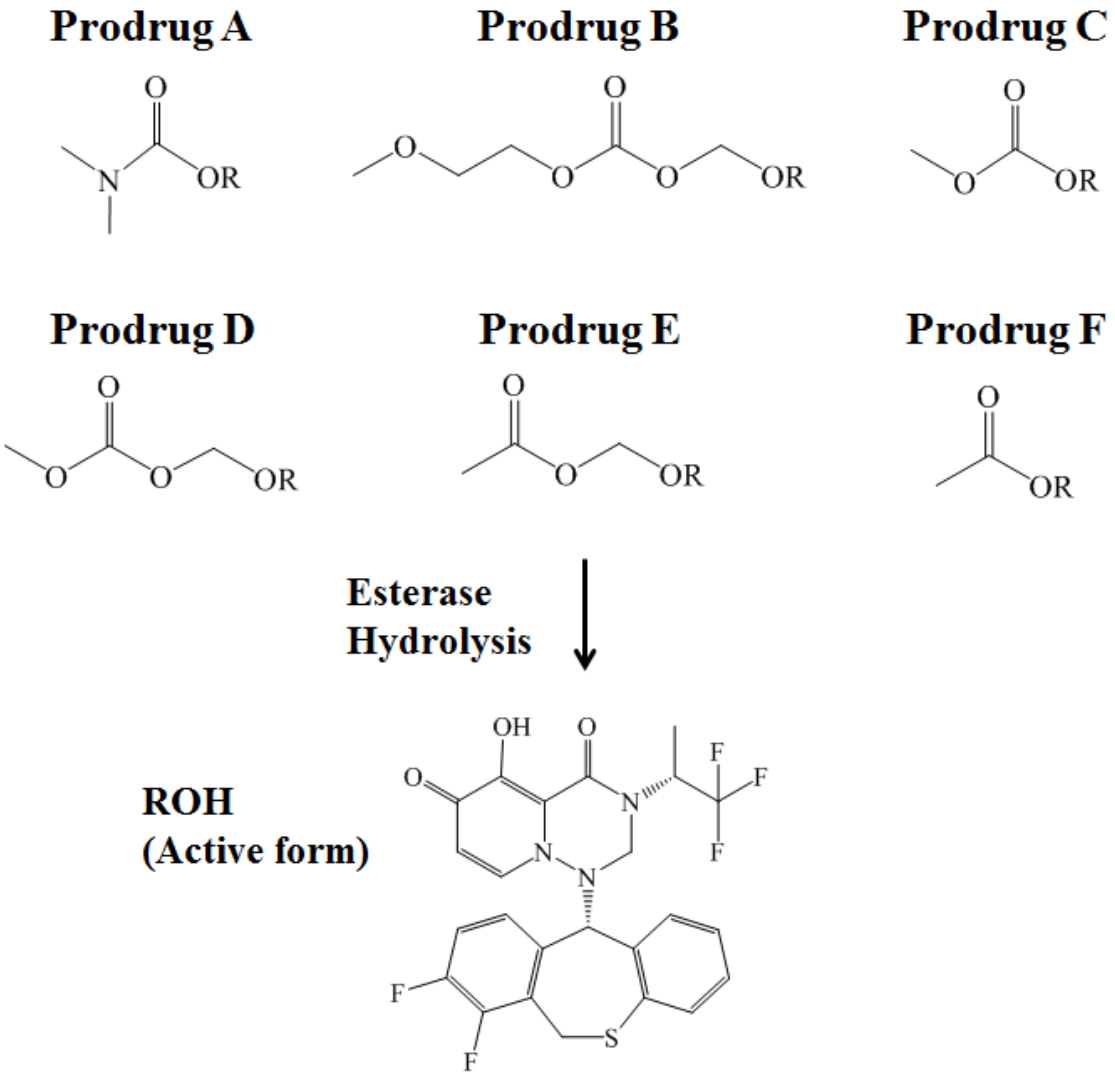

Fig. S1. Structures of six ester prodrugs and their hydrolysis into the active form by esterase. Six ester prodrugs (prodrugs A, B, C, D, E, and F) and their active form (ROH), the candidates of anti-influenza virus agents, are in-house compounds synthesized by Shionogi & Co., Ltd. These six prodrugs are all hydrolyzed into the same active form (ROH). The study of structure-activity relationships in the development of anti-influenza virus agents containing these compounds will be summited for publication.

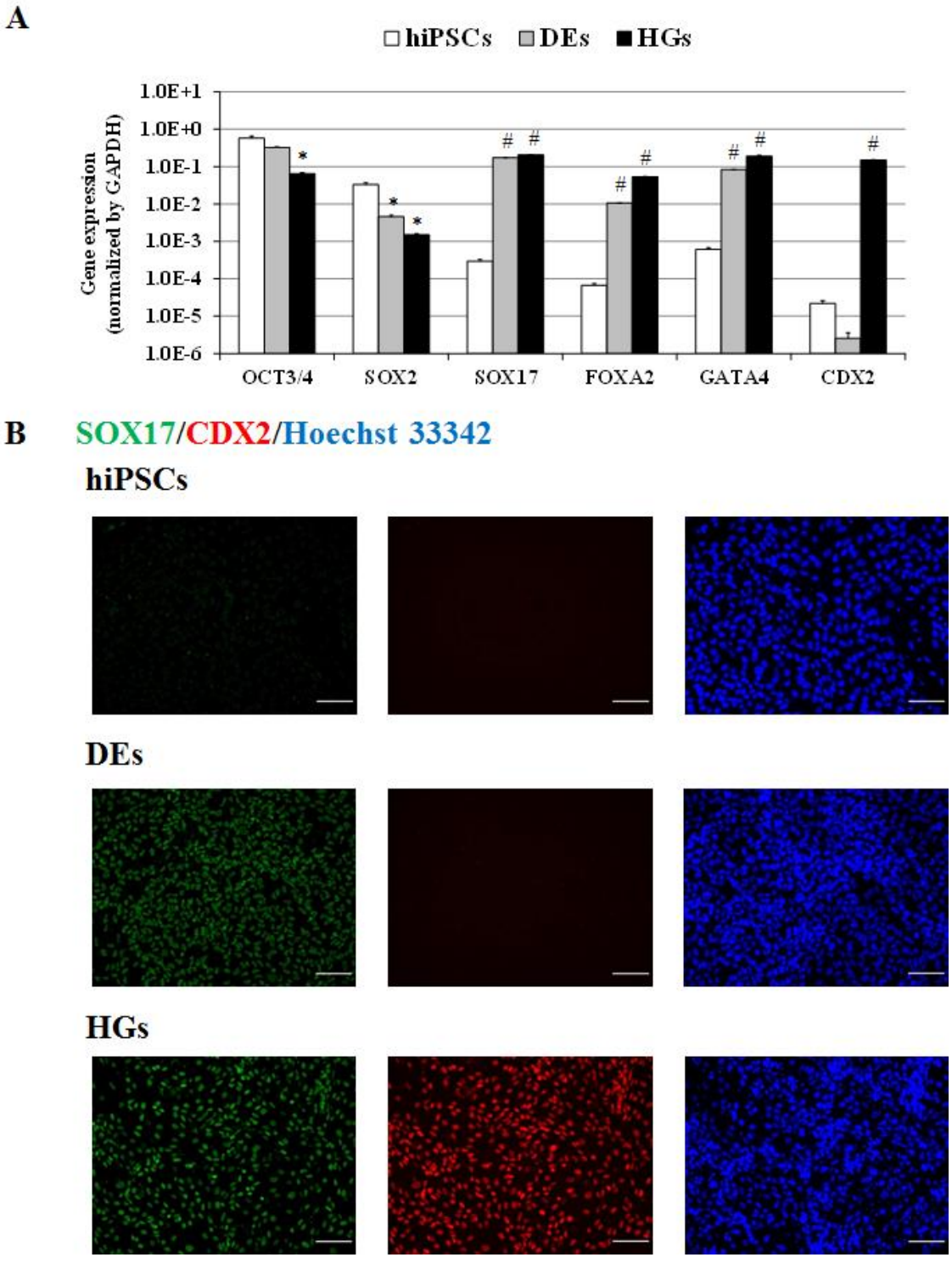

Fig. S2. Marker expressions in hiPSCs, differentiated DEs, and HGs.

HiPSCs were cultured in the presence of Activin A for 3 days to differentiate DEs, and

then the DEs was cultured in the presence of Wnt3a and FGF4 for 4 days to differentiate HGs. (A) Gene expression levels of undifferentiated markers (OCT3/4 and SOX2), DE markers (SOX17, FOXA2, and GATA4), a HG marker (CDX2) in hiPSCs, DEs, and HGs. Total RNA of each cell was extracted at each differentiated stage. Gene expression levels of markers were determined by qPCR analysis. Gene expression level of each marker was normalized by that of GAPDH and the relative expression ($2^{-\Delta Ct}$) calculated as described in Materials and Methods. Each data item represents the means (± S.E.M.) of triplicate analyses in a single sample. * and $^{\#}$ indicate significant difference of the quantitative value compared with hiPSCs (*$p < 0.05$; $^{\#}p < 0.01$). (B) Immunofluorescence analysis of SOX17 and CDX2 in hiPSCs, DEs, and HGs. Left (green), middle (red), and right (blue) panel showed staining of SOX17, CDX2 and Hoechst 33342, respectively. Scale bar represents 100 μm.

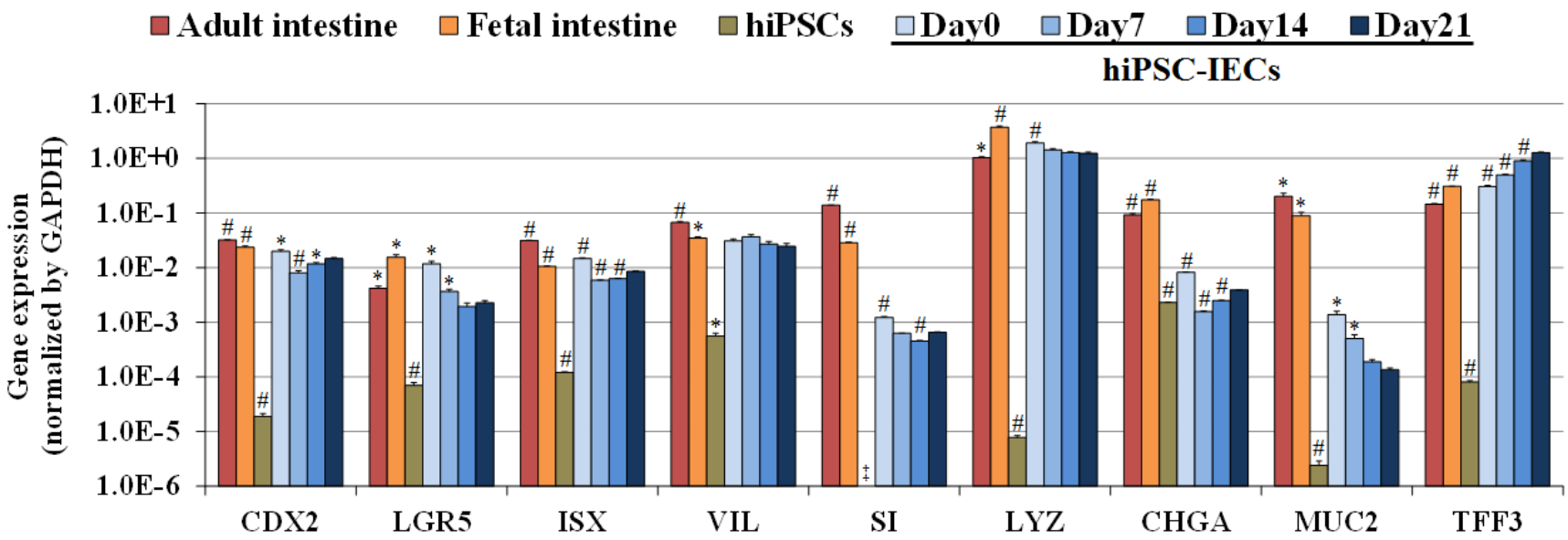

Fig. S3. Gene expression levels of intestinal markers in adult small intestine, fetal small intestine, hiPSCs, and hiPSC-IECs.

The gene expression levels of intestinal markers in adult small intestine (adult intestine), fetal small intestine (fetal intestine), hiPSCs, and hiPSC-IECs were examined by qPCR analysis as described in Materials and Methods section. The total RNAs of adult intestine and fetal intestine were purchased from Clonetech and BioChain Institute Inc., respectively. The total RNAs of hiPSCs and hiPSC-IECs were isolated using PureLink® RNA Mini Kit. hiPSC-IECs were cultured on Transwell inserts for defined periods; day 0 represents the cells before seeding on the Transwell insert, and day 7, day 14, and day 21 represent the cells cultured on the Transwell insert for 7, 14, and 21 days. The expression level of each gene was normalized by that of GAPDH, and the relative expression ($2^{-\Delta Ct}$) calculated as

described in Materials and Methods. Each data represents the means (± S.E.M.) of triplicate analyses in a single sample. * and # indicate significant difference of the quantitative value compared with day 21 (*$p < 0.05$; #$p < 0.01$). ‡The gene was not detected.

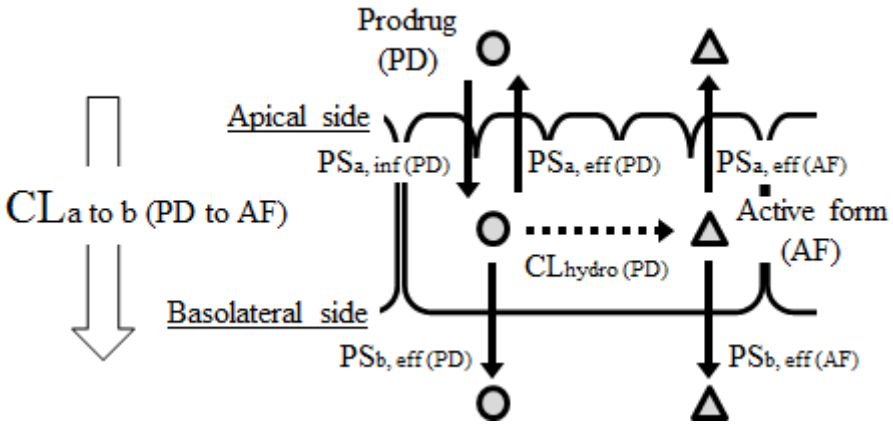

Fig. S4. Schematic diagram illustrating behavior of a prodrug around intestinal epithelial cells. $CL_{a\ to\ b\ (PD\ to\ AF)}$ is defined as the conversion clearance from a prodrug in the apical side to its active form in the basolateral side through the permeation and hydrolysis in intestinal epithelial cells. PS product is also defined as the product of the permeability coefficient and the surface area of plasma membrane of per intestinal epithelial cell in the present study. $PS_{a,\ inf\ (PD)}$, $PS_{a,\ eff\ (PD)}$, and $PS_{b,\ eff\ (PD)}$ represent the PS product for the apical influx, apical efflux, and basolateral efflux of a prodrug, respectively. $PS_{a,\ eff\ (AF)}$ and $PS_{b,\ eff\ (AF)}$ represent the PS product for the apical efflux and basolateral efflux of the active form, respectively. $CL_{hydro\ (PD)}$ represents the hydrolysis-mediated clearance of a prodrug into its active form in intestinal epithelial cell.

Table S1. Generic name of prodrugs A, B, C, D, E, and F and the active form

Compound	Generic name
Prodrug A	1-((S)-7,8-difluoro-6,11-dihydrodibenzo[b,e]thiepin-11-yl)-4,6-dioxo-3-((R)-1,1,1-trifluoropropan-2-yl)-2,3,4,6-tetrahydro-1H-pyrido[2,1-f][1,2,4]triazin-5-yl dimethylcarbamate
Prodrug B	((1-((S)-7,8-difluoro-6,11-dihydrodibenzo[b,e]thiepin-11-yl)-4,6-dioxo-3-((R)-1,1,1-trifluoropropan-2-yl)-2,3,4,6-tetrahydro-1H-pyrido[2,1-f][1,2,4]triazin-5-yl)oxy)methyl (2-methoxyethyl) carbonate
Prodrug C	1-((S)-7,8-difluoro-6,11-dihydrodibenzo[b,e]thiepin-11-yl)-4,6-dioxo-3-((R)-1,1,1-trifluoropropan-2-yl)-2,3,4,6-tetrahydro-1H-pyrido[2,1-f][1,2,4]triazin-5-yl methyl carbonate
Prodrug D	((1-((S)-7,8-difluoro-6,11-dihydrodibenzo[b,e]thiepin-11-yl)-4,6-dioxo-3-((R)-1,1,1-trifluoropropan-2-yl)-2,3,4,6-tetrahydro-1H-pyrido[2,1-f][1,2,4]triazin-5-yl)oxy)methyl methyl carbonate
Prodrug E	((1-((S)-7,8-difluoro-6,11-dihydrodibenzo[b,e]thiepin-11-yl)-4,6-dioxo-3-((R)-1,1,1-trifluoropropan-2-yl)-2,3,4,6-tetrahydro-1H-pyrido[2,1-f][1,2,4]triazin-5-yl)oxy)methyl acetate
Prodrug F	1-((S)-7,8-difluoro-6,11-dihydrodibenzo[b,e]thiepin-11-yl)-4,6-dioxo-3-((R)-1,1,1-trifluoropropan-2-yl)-2,3,4,6-tetrahydro-1H-pyrido[2,1-f][1,2,4]triazin-5-yl acetate
Active form	1-((S)-7,8-difluoro-6,11-dihydrodibenzo[b,e]thiepin-11-yl)-5-hydroxy-3-((R)-1,1,1-trifluoropropan-2-yl)-2,3-dihydro-1H-pyrido[2,1-f][1,2,4]triazine-4,6-dione

Table S2. Primer information in real-time RT-PCR using a TaqMan® Universal PCR Master Mix

Gege name	GenBank accession number	TaqMan Assay number
CYP3A4	NM_017460	Hs00430021_m1
CYP3A7	NM_000765	Hs00426361_m1
CES1	NM_001025195	Hs00275607_m1
CES2	NM_003869	Hs01077945_m1
UGT1A1	NM_000463	Hs02511055_s1
P-gp	NM_000927	Hs00184500_m1
BCRP	NM_004827	Hs01053790_m1
PEPT1	NM_005073	Hs00953898_m1
GAPDH (primer 1)	NM_002046	Hs02758991_g1

Table S3. Primer information in real-time RT-PCR using a One Step SYBR® PrimeScript™ PLUS RT-PCR Kit

Gege name	GenBank accession number	Primer sequence	
		Sense (5'→3')	Antisense (5'→3')
OCT3/4	NM_002701	TGAAGCTGGAGAAGGAGAAGCTG	GCAGATGGTCGTTTGGCTGA
SOX2	NM_003106	TGAGCGCCCTGCAGTACAA	GCTGCGAGTAGGACATGCTGTAG
SOX17	NM_022454	CTGCAGGCCAGAAGCAGTGTTA	CCCAAACTGTTCAAGTGGCAGA
FOXA2	NM_021784	GGTGTACTCCCGGCCCATTA	CAGAGTTAGCCGGGCCTGAA
GATA4	NM_001308093	TTACACGCTGATGGGACTGGAG	TCGGTGCTAGAAACACAATGCAA
CDX2	NM_001265	TTCACTACAGTCGCTACATCACC	CTGCGGTTCTGAAACCAGATT
LGR5	NM_003667	CAGCCATCAAGCAGGTGTTCA	ATGCTGGAATGTTTCAGGCTCA
ISX	NM_001303508	TCTCTAGCACCGCTGGATGAA	CTGCTACCCAAGTGATGAGCTACTG
VIL	NM_007127	GCTTGGCAACTCTAGGGACTGG	TGAGGTTGCTGTTAGCATTGAACAC
SI	NM_001041	AGACAACTATGCACGATGGGACAA	CATCCAGCGGGTACAGAGATGA
LYZ	NM_000239	GAGTTACACTCCACAACCTTGAACA	CCGTGATCCACAAGGCATTA
CHGA	HM_001275	TTGGAGAGCGAGGTCTTGGAG	TGCCTGTCAGCCAGGAATGT

MUC2	NM_002457	GATGCAAATGCTGGCATCAAAG	CAACCAGCACGTCATCCTGAA
TFF3	NM_003226	CTGCTGCTTTGACTCCAGGAT	CAGCTGGAGGTGCCTCAGAA
GAPDH (primer 2)	NM_002046	GCACCGTCAAGGCTGAGAAC	TGGTGAAGACGCCAGTGGA

Table S4. Conditions for LC-MS/MS analysis.

Compound	LC conditions					MS conditions	
	Instrument, column	Mobile phase A	Mobile phase B	Gradient condition Time (min); B concentration %	Flow rate (mL/min)	Instrument, Ionization Mode	SRM transition (m/z)
Transcellular transport studies across hiPSC-IECs							
Sulfasalazine	1, 1	0.1 % FA in water	MeCN	0-0.20 min; 20% → 0.50-0.90 min; 60% → 0.91-1.10 min; 95% → 1.11-1.40 min; 20%	0.75	1, Positive	399.1 /223.1
Midazolam	1, 1	0.1 % FA in water	MeCN	0-0.20 min; 20% → 0.50-0.90 min; 60% → 0.91-1.10 min; 95% → 1.11-1.40 min; 20%	0.75	1, Positive	326.1 /291.1
1-OH Midazolam	1, 1	0.1 % FA in water	MeCN	0-0.20 min; 20% → 0.50-0.90 min; 60% → 0.91-1.10 min; 95% → 1.11-1.40 min; 20%	0.75	1, Positive	342.1 /203.1
Irinotecan	1, 1	0.1 % FA in water	MeCN	0-0.20 min; 20% → 0.50-0.90 min; 60% → 0.91-1.10 min; 95% → 1.11-1.40 min; 20%	0.75	1, Positive	587.2 /543.1
SN38	1, 1	0.1 % FA	MeCN	0-0.20 min; 5% → 0.30-0.90 min; 40% →	0.75	1, Positive	393.2

		in water		0.91-1.10 min; 95% → 1.11-1.40 min; 5%			/263.0
Temocapril	1, 1	0.1 % FA in water	MeCN	0-0.10 min; 40% → 0.40-0.70 min; 80% → 0.71-0.90 min; 95% → 0.91-1.20 min; 40%	0.75	1, Positive	477.1 /270.0
Temocaprilat	1, 1	0.1 % FA in water	MeCN	0-0.10 min; 5% → 0.30-0.70 min; 70% → 0.71-0.90 min; 95% → 0.91-1.20 min; 5%	0.75	1, Positive	449.2 /190.1
Ganciclovir	1, 1	0.1 % FA in water	MeCN	0-0.10 min; 5% → 0.50-0.70 min; 20% → 0.71-0.90 min; 95% → 0.91-1.20 min; 5%	0.75	1, Positive	256.1 /152.1
Doxorubicin	1, 1	0.1 % FA in water	MeCN	0-0.10 min; 5% → 0.50-0.70 min; 90% → 0.71-0.90 min; 95% → 0.91-1.20 min; 5%	0.75	1, Positive	544.2 /397.0
Famotidine	1, 1	0.1 % FA in water	MeCN	0-0.20 min; 5% → 0.90-1.10 min; 95% → 1.11-1.40 min; 5%	0.75	1, Positive	338.0 /189.1
Sulpiride	1, 1	0.1 % FA in water	MeCN	0-0.10 min; 5% → 0.50-0.70 min; 60% → 0.71-0.90 min; 95% → 0.91-1.20 min; 5%	0.75	1, Positive	342.1 /112.1
Atenolol	1, 2	0.1 % FA in water	MeCN	0-0.20 min; 5% → 0.60-0.70 min; 80% → 0.71-1.00 min; 95% → 1.01-1.30 min; 5%	0.75	1, Positive	267.2 /190.1

Furosemide	1, 1	0.1 % FA in water	MeCN	0-0.10 min; 20% → 0.60-0.90 min; 60% → 0.91-1.10 min; 95% → 1.11-1.40 min; 20%	0.75	1, Negative	329.0 /284.9
Ranitidine	1, 1	0.1 % FA in water	MeCN	0-0.10 min; 5% → 0.50-0.70 min; 80% → 0.71-0.90 min; 95% → 0.91-1.20 min; 5%	0.75	1, Positive	315.1 /130.1
Hydrochlorothiazide	1, 1	0.1 % FA in water	MeCN	0-0.10 min; 5% → 0.50-0.70 min; 80% → 0.71-0.90 min; 95% → 0.91-1.20 min; 5%	0.75	1, Negative	295.9 /268.9
Acetaminophen	1, 1	0.1 % FA in water	MeCN	0-0.10 min; 5% → 0.50-0.70 min; 80% → 0.71-0.90 min; 95% → 0.91-1.20 min; 5%	0.75	1, Positive	152.1 /110.1
Propranolol	1, 1	0.1 % FA in water	MeCN	0-0.10 min; 25% → 0.60-0.70 min; 60% → 0.71-0.90 min; 95% → 0.91-1.20 min; 25%	0.75	1, Positive	260.2 /183.1
Antipyrine	1, 1	0.1 % FA in water	MeCN	0-0.20 min; 5% → 0.50-0.80 min; 80% → 0.81-1.00 min; 95% → 1.01-1.30 min; 5%	0.75	1, Positive	189.1 /56.1
Prodrug A	1, 3	0.1 % FA in water	MeCN	0-1.30 min; 50% → 0.31-1.50 min; 95% → 1.51-1.80 min; 50%	0.55	1, Positive	595.1 /247.0
Prodrug B	1, 3	0.1 % FA	MeCN	0-0.80 min; 53% → 0.81-1.30 min; 95% →	0.75	1, Positive	656.2

		in water		1.31-1.60 min; 53%			/247.0
Prodrug C	1, 3	0.1 % FA in water	MeCN	0-0.80 min; 53% → 0.81-1.30 min; 95% → 1.31-1.60 min; 53%	0.75	1, Positive	582.1 /247.1
Prodrug D	1, 3	0.1 % FA in water	MeCN	0-0.80 min; 53% → 0.81-1.30 min; 95% → 1.31-1.60 min; 53%	0.75	1, Positive	612.1 /247.1
Prodrug E	1, 3	0.1 % FA in water	MeCN	0-0.80 min; 53% → 0.81-1.30 min; 95% → 1.31-1.60 min; 53%	0.75	1, Positive	596.1 /247.0
Prodrug F	1, 3	0.1 % FA in water	MeCN	0-0.80 min; 53% → 0.81-1.30 min; 95% → 1.31-1.60 min; 53%	0.75	1, Positive	566.4 /247.1
Active form (condition 1)	1, 3	0.1 % FA in water	MeCN	0-1.30 min; 50% → 0.31-1.50 min; 95% → 1.51-1.80 min; 50%	0.55	1, Positive	524.1 /247.1
Active form (condition 2)	1, 3	0.1 % FA in water	MeCN	0-0.80 min; 53% → 0.81-1.30 min; 95% → 1.31-1.60 min; 53%	0.75	1, Positive	524.1 /247.1
Pharmacokinetics studies in rat							
Active form	2, 4	0.1 % FA	MeCN	0-0.90 min; 50% → 0.90-1.10 min; 95% →	0.75	2, Positive	524.0

(condition 3)		/ 0.05 % AA in water		1.11-1.40 min; 50%			/247.0
Active form (condition 4)	2, 4	0.1 % FA / 0.05 % AA in water	MeCN	0-0.20 min; 35% → 0.50-0.90 min; 60% → 0.90-1.10 min; 95% → 1.11-1.40 min; 35%	0.75	3, Positive	524.0 /247.0
Active form (condition 5)	2, 4	0.1 % FA / 0.05 % AA in water	MeCN	0 min; 45% → 0.60-0.80 min; 75% → 0.81-1.00 min; 45%	0.75	3, Positive	524.0 /247.0

Compounds were quantified by coupling a triple quadrupole mass spectrometer to a high-performance liquid chromatography (HPLC) or ultra-performance liquid chromatography (UPLC) system. Compounds were separated and eluted from the column under gradient conditions of mobile phase A and B; mobile phase A consisted of either 0.1 % of formic acid (FA) in water or 0.1% of FA and 0.05% acetylacetone (AA) in water, and mobile phase B consisted of acetonitrile (MeCN). The eluted compounds were detected by electrospray ionization using selected reaction monitoring (SRM) modes. The LC instruments used were either a Nexera X2 UHPLC system (Shimadzu, Kyoto, Japan; LC instrument 1) or an Acquity UPLC system (Waters; LC instrument 2). The LC columns used were YMC-Triart C18 column (2.1 mm × 50 mm, i.d., 3 μm; YMC, Ltd., Kyoto, Japan; column 1), CAPCELL PAK ADME column (2.1 mm

× 50 mm, i.d., 3 μm; Shiseido, Tokyo, Japan; column 2), L-column ODS (2.1 mm × 50 mm, i.d., 3 μm; Chemicals Inspection and Institute, Tokyo, Japan; column 3), or Acquity UPLC BEH C18 column (2.0 mm or 2.1 mm × 50 mm, i.d., 1.7 μm; Waters; column 4), and the all column temperatures were set at 40 C. The MS instruments used were a Triple Quad 6500 triple quadruple linear ion trap mass spectrometer (AB SCIEX, Framingham, MA; MS instrument 1), Quattro Ultima Pt (Waters; MS instrument 2), and API-5000 (AB SCIEX; MS instrument 3). The active form was measured under the following conditions. For the hydrolysis studies of prodrugs in hiPSC-IECs, condition 1 was employed in the study of prodrug A and condition 2 was employed in the studies of prodrugs B, C, D, E, and F. For the oral administration studies of prodrugs in rat, condition 3 was employed in the studies of prodrugs A and C, condition 4 was employed in the studies of prodrugs B, E, and F, and condition 5 was employed in the study of prodrug D. For the intravenous administration study of the active form in rat, condition 5 was employed.

Table S5. Hydrolysis activity in hiPSC-IEC monolayers and pharmacokinetic parameters in rats of six ester prodrugs.

Compound	Transcellular transport study across hiPSC-IEC monolayers	PK study in rat		
	CL_{int} (μL/min)	C_{max} (ng/mL)	AUC (ng×hr/mL)	BA (%)
Prodrug A	0.0239 ± 0.0056	13.5	134.7	4.1
Prodrug B	0.632 ± 0.040	141	1777	54.3
Prodrug C	0.655 ± 0.037	59.4	730	22.3
Prodrug D	0.690 ± 0.055	72.9	929	28.4
Prodrug E	1.11 ± 0.06	104	1242	38.0
Prodrug F	1.66 ± 0.13	172	2045	62.5

CL_{int}, a parameter of hydrolysis activity of ester prodrugs into the active form, was determined by means of the apical-to-basolateral transcellular transport study in hiPSC-IECs as described in Materials and Methods. The pharmacokinetic parameters (C_{max}, AUC, and BA) of six prodrugs in rats were calculated from the plasma concentrations of the active form after oral administrations of six prodrugs and intravenous administration of the active form. Six ester prodrugs and the active form are in-house compounds synthesized by Shionogi & Co., Ltd., and these six prodrugs are all hydrolyzed into the same active form. Each value of CL_{int} in hiPSC-IECs represents

the mean ± S.E.M. of three determinations. Each value of C_{max}, AUC, and BA in rat represents the mean of two or three rats.

Table S6. Prediction of human Fa of values 14 drugs from their P_{app} values across hiPSC-IEC monolayers.

Compound	P_{app} in hiPSC-IECs ($\times 10^{-6}$ cm/sec)	Predicted Fa	Observed Fa			
			Median	Zhao et al. (2001)	Sugano et al. (2002)	Verma et al (2010)
Ganciclovir	0.0175 ± 0.0025	0.05	0.06	0.03	0.03	0.09
Doxorubicin	0.0758	0.20	0.12	0.007-0.23	not examined	0.12
[^{14}C]Mannitol	0.222 ± 0.020	0.48	0.16	0.16	0.16	not examined
Famotidine	0.160 ± 0.030	0.38	0.38	0.38	0.38	not examined
Sulpiride	0.0795 ± 0.0010	0.21	0.40	0.44	0.35	0.44
Atenolol	0.0972 ± 0.0016	0.25	0.50	0.50	0.50	0.50
Sulfasalazine	0.221 ± 0.027	0.48	0.59	0.56-0.61	not examined	0.59
Furosemide	0.467 ± 0.098	0.75	0.61	0.61	0.61	0.61
Ranitidine	0.0637 ± 0.0026	0.17	0.64	0.39-0.88	0.50	0.65
Hydrochlorothiazide	0.474 ± 0.119	0.75	0.69	0.65-0.72	not examined	not examined
[^{3}H]Digoxin	1.81 ± 0.04	1.00	0.81	0.81	not examined	0.81
Acetaminophen	17.1 ± 0.4	1.00	0.90	0.80	0.80	1.00

Propranolol	39.3 ± 0.3	1.00	0.95	0.99	0.90	0.99
Antipyrine	23.9 ± 2.5	1.00	0.97	0.97	0.97	0.97

The P_{app} values of 14 drugs were determined by means of the apical-to-basolateral transcellular transport study across hiPSC-IECs. The data of doxorubicin represent the mean of duplicate experiments, and the data of 13 other drugs represent the mean ± S.E.M. of triplicate experiments. Human Fa values were taken from the literature (Zhao et al., 2001; Sugano et al., 2002; Varma et al., 2010). If multiple Fa values are reported in these literatures, the median value was calculated and used. The predicted Fa values were calculated by using Eq. 9 as described in Results.

Reference for Supplemental Data

Hashimoto K, Matsunaga N and Shimizu M (1994) Effect of vegetable extracts on the transepithelial permeability of the human intestinal Caco-2 cell monolayer. *Bioscience, biotechnology, and biochemistry* **58:**1345-1346.

Higgins CF and Linton KJ (2004) The ATP switch model for ABC transporters. *Nat Struct Mol Biol* **11:**918-926.

Rubio-Aliaga I and Daniel H (2008) Peptide transporters and their roles in physiological processes and drug disposition. *Xenobiotica* **38:**1022-1042.

Spence JR, Mayhew CN, Rankin SA, Kuhar MF, Vallance JE, Tolle K, Hoskins EE, Kalinichenko VV, Wells SI, Zorn AM, Shroyer NF and Wells JM (2011) Directed differentiation of human pluripotent stem cells into intestinal tissue in vitro. *Nature* **470:**105-109.

Sugano K, Takata N, Machida M, Saitoh K and Terada K (2002) Prediction of passive intestinal absorption using bio-mimetic artificial membrane permeation assay and the paracellular pathway model. *Int J Pharm* **241:**241-251.

Varma MV, Obach RS, Rotter C, Miller HR, Chang G, Steyn SJ, El-Kattan A and Troutman MD (2010) Physicochemical space for optimum oral bioavailability: contribution of human intestinal absorption and first-pass elimination. *J Med Chem* **53:**1098-1108.

Zhao YH, Le J, Abraham MH, Hersey A, Eddershaw PJ, Luscombe CN, Butina D, Beck G, Sherborne B, Cooper I and Platts JA (2001) Evaluation of human intestinal absorption data and subsequent derivation of a quantitative structure-activity relationship (QSAR) with the Abraham descriptors. *J Pharm Sci* **90:**749-784.